polymer papers

Regime III crystallization in melt-crystallized polymers: The variable cluster model of chain folding

John D. Hoffman*

National Measurement Laboratory, National Bureau of Standards, Washington, DC 20234, USA

(*Received* 25 *March* 1982; *revised* 5 *April* 1982)

The kinetic nucleation theory of chain folding, including the effects of reptation, is extended to predict the increase in crystal growth rate G that is implied by measurements on PE and POM at moderately large undercoolings. The increased growth rate denotes the rather abrupt transition from Regime II where $G \propto i^{1/2}$ to Regime III where $G \propto i$ (i = surface nucleation rate). The distance between the niches on the growth front in Regime II diminishes rapidly with falling crystallization temperature T_x, and approaches the molecular width at a specified undercooling where Regime III begins. In PE, the Regime I→Regime II transition occurs at $\Delta T \simeq 16°C$, and the Regime II→Regime III transition is predicted to occur at $\Delta T \sim 23°C$ (ΔT based on $T_m^\circ(\infty) = 145°C$). Growth rate data on PE and POM crystallized from the melt suggest conformity with the theoretical predictions. The implications of Regime III crystallization to chain morphology are discussed. The kinetic theory, which predicts narrowly spaced niches on the growth front, taken together with the restrictions on the degree of non-adjacent re-entry imposed by the 'Gambler's Ruin' treatment, leads directly to the 'variable cluster' model as the relevant morphology in Regime III. Here runs of adjacently chain-folded stems of varying size (averaging about three or so stems) are laid down interspersed with non-adjacent re-entries, leading to a lamellar surface that is about two-thirds 'regular' or 'tight' folds, most or all of these representing strictly adjacent re-entries. The steady-state reptation process operative in Regimes I and II in PE is impaired at temperatures just below the inception of Regime III, and it is suggested that at lower temperatures the 'slack' portions of the chains engage in forming the small clusters of adjacent stems. The variable cluster model leads in a natural way to the amorphous component found in quench-crystallized polymers, and is consistent with neutron scattering data on quench-crystallized PEH–PED.

Keywords Regime III; crystallization; chain fold; reptation; polyethylene; poly(oxymethylene); variable cluster model; nucleation theory; neutron scattering; Gambler's Ruin problem

INTRODUCTION

The kinetic theory of polymer crystallization with chain folding has been attended by considerable success in understanding and interpreting data on melt-crystallized linear polymers. With an exception that will be treated here, the shape of the spherulite or axialite growth rate curves as a function of temperature and molecular weight can be interpreted in quantitative terms, and values of the fold surface free energy and work of chain folding can be derived from these kinetic measurements that are in reasonable accord with independent theoretical and experimental determinations of these quantities[1,2]. Much of the latter success results from the recognition of the distinction between Regime I and Regime II crystallization. The existence of the Regime I→Regime II transition at $\Delta T_t \cong 16 \pm 1°C$ has been demonstrated[2,3] for a number of polyethylene (PE) fractions ranging in molecular weight M_z from 2.65×10^4 to 2.04×10^5. (In quoting this undercooling for the Regime I→Regime II transition, we have assumed that $T_m^\circ(\infty) = 145°C$.) In Regime I, which occurs nearest the melting point, the observable growth rate G is proportional to the surface nucleation rate i, while in the lower temperature Regime II it is proportional to $i^{\frac{1}{2}}$. Also, the general nature of the change of the initial lamellar thickness with temperature is successfully predicted insofar as it can be tested, the complication being that the lamellae often tend to spontaneously thicken even during their formation[1,3]. The attendant melting behaviour of the thin lamellae is also generally understood when isothermal thickening, and melting out and recrystallization on warming, are taken into account[1]. Perhaps most important of all, the kinetic theory[1,2], taken together with the restrictions on non-adjacent re-entry given in the Gambler's Ruin treatment[4] of lamellar morphology, will serve to provide considerable insight into the mode of formation and molecular conformation present in the largely chain-folded lamellar entities that are widely observed in polymers crystallized from the melt. More will be said concerning this latter point in the present paper.

The exception mentioned above is that an abrupt change of slope in the growth rate *versus* temperature curves is sometimes found at relatively low crystallization temperatures (i.e., moderately large undercoolings) that is just the reverse of that predicted for the Regime I→Regime II transition. At the I→II transition, the slope of the growth rate *falls off* with lowering temperature, while in the exceptions mentioned the slope at the transition *increases*. This latter effect will later be iden-

* Present address: Department of Chemical and Nuclear Engineering, University of Maryland, College Park, Maryland 10742, USA

0032-3861/83/010003-24$03.00

tified as the Regime II→Regime III transition. The rate of crystal growth data of Pelzbauer and Galeski[5] on poly(oxymethylene) (POM) clearly show the existence of a Regime II→Regime III transition, and their results will be analysed in detail. Also it will be brought out that the recent low temperature growth rate studies of Barham, Jarvis and Keller[6] provide considerable support for the existence of a Regime II→Regime III transition in PE. Thus, with the development of the Regime III treatment, the applicability of nucleation theory is extended to substantially lower crystallization temperatures than before.

Regime III crystallization is clearly implied by the previously extant[2] theory for Regimes I and II. In Regime I, one surface nucleus causes the completion of the entire substrate of length L. These nuclei are deposited sporadically in time on the substrate at a rate i per unit length in a manner that is highly dependent on temperature, the rate increasing rapidly as the temperature is lowered, i.e. as the undercooling ΔT is increased[1,2]. Substrate completion at a rate g begins at the energetically favourable niche that occurs on either side of a surface nucleus. In Regime II, multiple surface nuclei begin to occur on the substrate because of the rapid increase of i associated with the larger undercooling[1,2]. It will emerge that nucleation theory is explicit on the mean separation of these surface nuclei, and this defines the niche separation with suitable accuracy. Regime III is entered when the niche separation characteristic of the substrate in Regime II approaches the width of a stem. Here the postulates underlying the Regime II theory become invalid, and it is this circumstance that gives rise to Regime III. It will be shown that in Regime III the crystal growth rate is controlled by the rate of deposition of nuclei on the substrate i, rather than $i^{\frac{1}{2}}$ as in Regime II. It is this situation that leads to the upswing in the growth rate as the system passes with descending crystallization temperature from Regime II to Regime III.

There are a number of consequences associated with Regime III crystallization that have a significance well beyond the prediction of the shape of growth rate curves as a function of temperature.

The kinetic theory provides useful guidelines concerning the nature of the chain morphology that must occur in Regime III, especially when considered together with the upper limit of the probability of non-adjacent re-entry, p_{nar}. Because of the presence of a quite short effective substrate length in Regime III arising from the proximity of the niches, the kinetic theory clearly implies that a molecule crystallizes in the form of small sets of stems on the rough growth front. We note also that Regime III, with its abundance of closely spaced niches, invites non-adjacent re-entry on a large scale in a lamellar system. Thus in one sense Regime III crystallization represents a 'worst case' for regular chain folding. There are however strong restrictions on p_{nar}, and a recent rigorous theoretical analysis ('Gambler's Ruin' problem) by Guttman *et al.*[4] shows that the upper bound of p_{nar} is $\sim 1/3$ for a lamellar system without a very large tilt of the chain axes with respect to the fold plane. Thus, the Gambler's Ruin treatment demands that the probability of 'tight' or 'regular' folds, p_{tf}, is $\sim 2/3$ as a lower bound for such a system. This limit arises from the necessity of avoiding a density paradox at the lamellar surface, such as is exhibited by (and which invalidates) the 'random switchboard' model. The 'variable cluster' model emerges in a natural way from these considerations. Here a molecule laid down in the Regime III process will exhibit sets of small clusters, the adjacent stems in each cluster being connected by tight folds. The clusters are connected to each other by non-adjacent re-entry events; the probability of 'regular' or 'tight' folding, p_{tf}, is $\sim 2/3$ for the system as required by the Gambler's Ruin treatment, and many of the tight folds in each cluster will represent strictly adjacent re-entries. This part of the discussion has added significance because neutron scattering experiments[7] aimed at determining chain morphology in quench-crystallized PEH–PED mixtures have been conducted on specimens formed either deep in Regime II or more likely just in Regime III. These and related points will be discussed, and it will be noted that the variable cluster model is consistent with the radius of gyration, mean cluster size, and scattering intensity that is obtained from neutron scattering data on quench-crystallized PEH–PED. It will also be shown that the variable cluster model is fully consistent with the degree of crystallinity observed near the inception of Regime III in PE.

There has been much discussion concerning whether the 'random switchboard' or the 'regularly folded' model was the 'correct' representation of the lamellae in a melt-crystallized polymer. The author is an unrepentant advocate of the 'regularly folded' model as a starting point for calculations of the surface free energy, rate of growth, and initial lamellar thickness in such systems; despite its deficiencies, the 'regularly folded' model is fully justified as a reasonable first approximation by the clear-cut and verifiable results that it yields in connection with the centrally important properties just mentioned, and by the Gambler's Ruin treatment which shows that the lamellar surface must consist of about two-thirds 'tight' folds when the stems are not strongly tilted. ('Tight' folds do not contribute to the amorphous phase, and are mostly or entirely associated with adjacent re-entry). The strictly regularly folded model does not accomodate the presence of an amorphous phase, because in its extreme form non-adjacent events are not considered. It has been pointed out before (for instance in references 1 and 2) how the introduction of some non-adjacent events will lead to an amorphous component in a more general chain fold model, and in the present paper such events are considered explicitly in connection with Regime III crystallization. The result is that an amorphous phase consisting mainly of random-coil loops connecting non-adjacent re-entries is predicted outright; the kinetic picture is but little changed from that of the strictly regularly folded model, largely because non-adjacent events are restricted by the Gambler's Ruin treatment to about only one in three. Concerning the issue of the correctness of the regularly folded model, as opposed to the random switchboard model, it is of course our view that neither is strictly correct. However, evidence will be cited in the present paper showing that the 'regularly folded' model is considerably closer to the true state of affairs as regards the degree of 'tight' or 'regular' folding; its usefulness as a vehicle for the calculation of the lamellar thickness, kinetics of growth, and surface free energy is already well-known and this will become further apparent here. In its more general form to be discussed here, which entails a limited degree of non-adjacent re-entry as bounded by the Gambler's Ruin treatment, it is capable of organizing an even larger body of experimental knowledge.

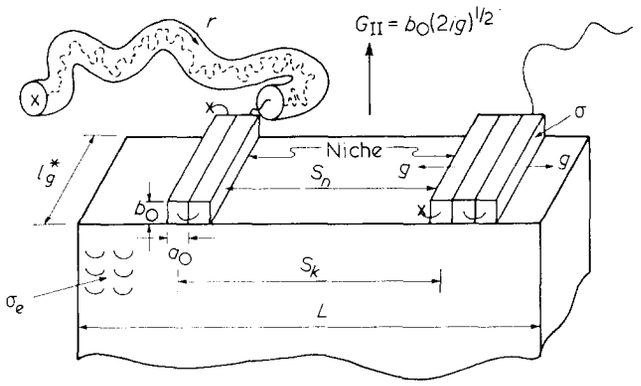

Figure 1 Model for Regime II growth showing multiple nucleation (schematic). S_k represents the mean separation between the primary nuclei, and S_n denotes the mean distance between the associated niches. The primary nucleation rate is i, and the substrate completion rate is g. The overall observable growth rate G_{II} resulting from primary nucleation and substrate completion is given by $b_0(2ig)^{1/2}$. Reptation tube contains molecule being reeled at rate r onto substrate by force of crystallization

Returning now to the specific points considered in this paper, it will be shown that the initial stem length l_g^* in Regime III is essentially a continuation of that exhibited in Regimes I and II. There are certain provisos attached to this prediction that will be noted in due course. In the specific case of POM, it is shown that the experimental estimate of the initial lamellar thickness is consistent with that calculated from the theoretical expression for l_g^* using the fold surface free energy determined from an analysis of the growth kinetics in both Regimes II and III.

It has been demonstrated previously that 'steady state' reptation is the subcooled melt is rapid enough in Regimes I and II in PE to allow a fraction of each pendant chain to be reeled through the interentangled melt onto the growth front with adjacent re-entry or 'tight' folding, resulting in a lamellar morphology that is about two-thirds or more tight folds, most of these tight folds representing adjacent re-entries[2]. It will be shown here that steady-state reptation is rapid enough in PE in the subcooled melt to permit adjacent re-entry in the small clusters formed in Regime III at temperatures just at its inception. This calculation makes it clear however that the steady state reptation process characteristic of Regimes I and II is not rapid enough at lower temperatures to sustain the formation of even such small clusters. It is postulated that the concept of 'slack' or 'stored length'[8,9] provides a mechanism that allows rapid transport of enough chain segments to form small clusters with chain folding in the main part of Regime III. A brief discussion is given of the effects that may occur in specimens of very high molecular weight and at low crystallization temperatures in Regime III.

NICHE SEPARATION THEORY

The treatment to follow is patterned after that given more briefly in a recent *Discussion of the Faraday Society*[10]. The version given here is more exact in a number of respects. The separation between the 'niches' exhibited in Regime II is the key to understanding the onset of Regime III at higher undercoolings. The basic situation treated is shown in *Figure 1*. In Regime II numerous nuclei form on the substrate at a rate i, and each nucleus possesses two niches that promote rapid completion of the substrate at a rate g. The resultant observable growth rate is[11] $G_{II} = b_0(2ig)^{\frac{1}{2}}$, where b_0 is the layer thickness (*Figure 1*).

The number of nucleation sites per cm in Regime II is (*cf.* refs. 2 and 10)

$$N_k = (i/2g)^{\frac{1}{2}} \tag{1}$$

and the mean separation between the sites is

$$S_k = 1/N_k = (2g/i)^{\frac{1}{2}} \tag{2}$$

The task now at hand is to evaluate i and g in terms of nucleation theory. This will serve to show that S_k rapidly approaches the dimensions of the stem width at a certain undercooling in Regime II, which signals the onset of Regime III. Previous mention of this phenomenon may be found elsewhere[10,12].

In the material that ensues, frequent reference will be made to a recent and improved treatment of surface nucleation and substrate completion with reptation that features a more exact evaluation of the pre-exponential factors in each[2].

The nucleation rate on the substrate is given by[2]

$$i(\text{nuclei}\cdot\text{cm}^{-1}\cdot\text{s}^{-1}) = S_T/a_0 n_s = (N_0 \beta_g p_i/a_0 n_s) e^{-4b_0\sigma\sigma_e(\Delta f)kT} \tag{3a}$$

where the effective number of reacting species N_0, is

$$N_0 = (\bar{z}n_s)(C_n P_0) \tag{3b}$$

and $(\bar{z}n_s)$ is the number of $-CH_2-$ units on the growth front, C_n a coordination number that is ~ 4, and P_0 the configurational path degeneracy. The quantity P_0 takes on values[2] of unity to upwards of 25 (see later).

The retardation factor resulting from the necessity of moving the polymer chain through the melt by steady-state reptation onto the substrate is[2,10]

$$\beta_g(\text{event}\cdot\text{s}^{-1}) = (\kappa/n)(kT/h) e^{-Q_b^{\ddagger}/RT} \tag{3c}$$

The numerical constant p_i, which for PE is about five, is given by

$$p_i = kT/2l_u b_0 \sigma \tag{3d}$$

In the above expressions, S_T is the total flux, a_0 the molecular width, b_0 the layer thickness, so that the cross-sectional area of the chain is $A_0 = a_0 b_0$ cm^2, and n_s the number of stems of width a_0 that constitute the substrate length L (see *Figure 1*). The symbol σ represents the lateral surface free energy in erg cm^{-2} (1 erg cm^{-2} = 1 millijoule m^{-2}), and σ_e the fold surface free energy $\sigma_e = q/2A_0$ in the same units, q being the work of chain folding. The quantity $\bar{z}$ is the number of chain units each of length l_u that go to make up the lamellar thickness l_g^*, i.e., $\bar{z} = l_g^*/l_u$. The quantity Δf is the driving force for crystallization in erg cm^{-3}, which may be approximated as

$$\Delta f = (\Delta h_f)(\Delta T)/T_m^{\circ} \tag{3e}$$

where Δh_f is the heat of fusion in erg cm^{-3}, ΔT the undercooling, and T_m° the equilibrium melting point relevant to a very large crystal of the molecular weight

under consideration; closer approximations for Δf are available[1], but the one just given is sufficient for the present purpose. In equation (3c) n is the number of chain units in the dangling chain in the melt that is being reptated onto the crystal surface. As a conservative approximation we shall take n to be the number of chain units corresponding to the molecular weight of the fraction under consideration. The quantity Q_D^* is the activation energy of the steady-state reptation process in the melt, which is quoted by Klein and Briscoe to be about 7000 cal mol^{-1} for PE[13] (1 cal = 4.187 j). The quantity κ is a numerical constant in the range of about 1 to 10 that can be determined by experiment[2]. The factor $\exp(-Q_D^*/RT)$ can be replaced by $\exp[-U^*/R(T-T_\infty)]$ where appropriate (see later).

Consider now the expression for the substrate completion rate g. For the case $\psi = 0$, this is given by[2]

$$g(\text{cm}\cdot\text{s}^{-1}) \equiv a_0(\mathbf{A}-\mathbf{B}) = a_0 f \beta_g e^{-q/kT} = a_0 f(\kappa/n)(kT/h)e^{-Q_D^*/RT}e^{-q/kT} \quad (4a)$$

where q is the work of chain folding as before, and the numerical factor f, which for polyethylene is close to 0.5, is

$$f \cong a_0(\Delta f)/\sigma = a_0(\Delta h_f)(\Delta T)/\sigma T_m^\circ. \quad (4b)$$

Notice that both the necessity of forming chain folds and the reptation process in the melt exert retardations on the substrate completion process, as is shown by the presence of the factors $\exp(-q/kT)$ and $\beta_g \propto \exp(-Q_D^*/RT)$, respectively. (Later an expression for g will be given for $\psi \neq 0$ that gives similar though somewhat larger numerical results for allowable values of ψ, which range from zero to about one-third). The factor $1/n$ in β_g is present explicitly because the molecule must be reeled through the melt onto the substrate by the force of crystallization, the resistance being associated with the friction coefficient arising from steady-state reptation, which is proportional to n. It is this factor that leads to the $1/M$ molecular weight dependence of the pre-exponential factors in Regimes I and II[2].

It follows from the above that the mean separation of the nuclei S_k on the substrate in Regime II, where multiple nucleation occurs, is

$$S_k(\text{cm}) = \left[\frac{a_0 l_u(\Delta h_f)(\Delta T)}{T_m^\circ}\right] \times \left[\frac{2A_0\exp(-q/kT)}{(C_nP_0)\sigma_e kT}\right]^{\frac{1}{2}} e^{K_{g(\text{II})}/T(\Delta T)} \quad (5a)$$

where $K_{g(\text{II})}$ is the experimentally known quantity $2b_0\sigma\sigma_e T_m^\circ/(\Delta h_f)k$ (see below). Equation (5a) replaces an earlier[10] and less accurate expression for S_k. In deriving equation (5a) the simplification $\bar{z} = l_g^*/l_u \cong 2\sigma_e T_m^\circ/(\Delta h_f)(\Delta T)l_u$ was employed. Observe that it is not necessary to know κ, Q_D^* (or U^* and T_∞) to estimate S_k. The actual mean separation of the niches, S_n, will be somewhat smaller than S_k, and we employ the approximation

$$S_n \cong S_k - a_0 \quad (5b)$$

in the calculations to follow. The value of S_n may be slightly smaller than that given by equation (5b) because of growth in the g direction, but this has no effect on the general physical interpretation.

Before proceeding with an illustrative calculation of S_n for PE showing the onset of Regime III, it is useful to cite the properties of Regimes I and II. The overall (observable) growth rate G_{II} in Regime II is[2]

$$G_{\text{II}} = b_0(2ig)^{\frac{1}{2}} = \left(\frac{C_{\text{II}}}{n}\right)e^{-Q_D^*/RT}e^{-K_{g(\text{II})}/T(\Delta T)} \quad (6a)$$

where

$$K_{g(\text{II})} = 2b_0\sigma\sigma_e T_m^\circ/(\Delta h_f)k \quad (6b)$$

and

$$C_{\text{II}} = (2p_i f)^{\frac{1}{2}}(C_nP_0)^{\frac{1}{2}}\kappa(kT/h)b_0\bar{z}^{\frac{1}{2}}e^{-q/2kT}. \quad (6c)$$

The corresponding quantities for Regime I are[2]

$$G_{\text{I}} = b_0 i n_s a_0 = \left(\frac{C_{\text{I}}}{n}\right)e^{-Q_D^*/RT}e^{-K_{g(\text{I})}/T(\Delta T)} \quad (7a)$$

where

$$K_{g(\text{I})} = 4b_0\sigma\sigma_e T_m^\circ/(\Delta h_f)k \quad (7b)$$

and

$$C_{\text{I}} = \kappa p_i(kT/h)(C_nP_0)b_0(\bar{z}n_s). \quad (7c)$$

Observe that according to the theory that $K_{g(\text{I})} = 2K_{g(\text{II})}$; this has been shown to hold experimentally to a good approximation for PE fractions[2]. Also, the pre-exponential factors are in good accord with experiment[2]. The Lauritzen 'Z test' expression $Z = iL^2/4g$ describes the undercooling where the Regime I→Regime II transition takes place[2,11]. For PE specimens of moderately high molecular weight ($M_z = \sim 30\,000$ to $\sim 200\,000$), the Regime I→Regime II transition takes place at about 127° to 128°C[2,3], or $\Delta T \cong 16$°C if $T_m^\circ(\infty)$ is set at 145°C. The transition between Regime II and Regime III is predicted to take place at a considerably larger undercooling (see below).

It is now possible to utilize equations (5) to calculate the niche separation as a function of undercooling in a manner that brings out the existence of Regime III. PE will be used as an example. We choose to measure ΔT from $T_m^\circ(\infty) = 145$°C, and utilize the following values of the parameters[2] in equation (5): $a_0 = 4.55 \times 10^{-8}$ cm, $l_u = 1.27 \times 10^{-8}$ cm, $\Delta h_f = 2.8 \times 10^9$ erg cm^{-3}, $C_nP_0 = 100$, $T_m^\circ = 145$°C = 418.2 K, $A_0 = 18.9 \times 10^{-16}$ cm^2, $q = 4900$ cal mol^{-1}, $\sigma_e = 90$ erg cm^{-2}, and $K_{g(\text{II})} = 0.900 \times 10^5$ K^2, the latter being the directly observed experimental value. This yields

$$S_k(\text{cm}) \cong S_n + a_0 = 5.45 \times 10^{-13}(\Delta T)e^{0.900 \times 10^5/T(\Delta T)}. \quad (8)$$

The foregoing parameters are consistent with $C_{\text{I}} = 5.00 \times 10^{13}$, $C_{\text{II}} = 3.34 \times 10^7$, $K_{g(\text{I})} = 2K_{g(\text{II})} = 1.800 \times 10^5$ K^2 which can be derived from rate data on PE fractions under the condition $K_{g(\text{I})} = 2K_{g(\text{II})}$[2].

Figure 2 depicts the mean separation of the sites S_k and the mean niche separation S_n as a function of undercooling calculated with equation (8). Previous calculations made under the condition $K_{g(\text{I})} = 2K_{g(\text{II})}$ have shown that the Regime I→Regime II transition takes place at

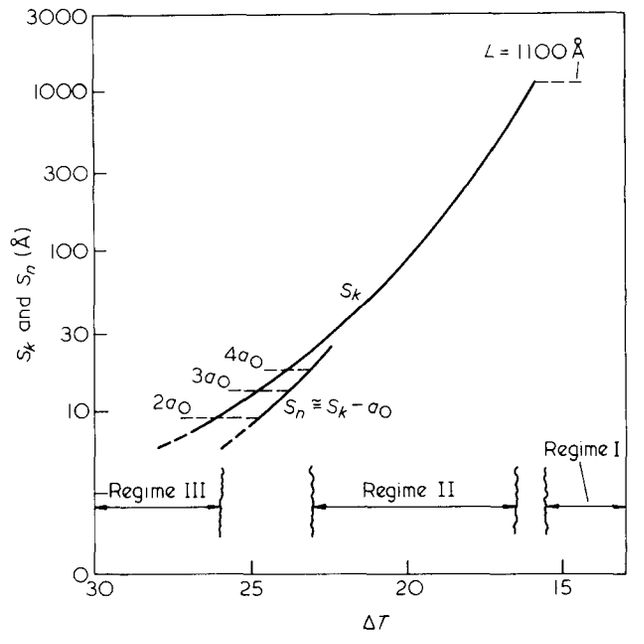

Figure 2 Nucleation site separation S_k and niche separation S_n as a function of undercooling for polyethylene. Solid lines calculated according to equation (8). See text for details. $T_m^0(\infty)$ was taken as 145°C

$\Delta T \cong 16$°C where the corresponding ratio C_I/C_{II} determines that $L \cong 0.11$ μm^2. At lower undercoolings than this, the nucleation rate i is so slow that the substrate has only one nucleus. At larger undercoolings than $\Delta T \cong 16$°C, multiple nucleation occurs on the substrate, and the above formula for S_k and S_n is then applicable. As the undercooling is increased above $\Delta T \cong 16$°C, the niche separation falls rapidly, and approaches the width of a molecule a_0. The rapid drop in S_n and S_k is a result of the great increase in the surface nucleation rate as expressed by the factor $\exp[K_{g(II)}/T(\Delta T)]$. At $\Delta T = 23.2$°C, S_n is $4a_0$, and at $\Delta T = 24.8$°C, it is only $2a_0$ (*Figure 2*).

Under the conditions where S_n approaches the molecular width a_0, the assumptions underlying the Regime II process become invalid, since substrate completion at a rate g is highly rectricted. Crystallization at larger undercoolings than $\Delta T \cong 23°$ to 25°C must take place under a different law than that which governs Regime II. Earlier it was suggested that the overall growth rate in Regime III was proportional to i rather than $i^{1/2}$ as it is in Regime II[12]. From the foregoing we must expect Regime II to begin in PE at a ΔT of roughly 23° to 25°C, corresponding to crystallization temperatures of about 119°C to 121°C for fractions of moderate molecular weight. (Subsequently, we shall mention circumstances that might allow the II→III transition to be as low as about 117°C). The prediction of the temperature at which Regime III will begin is relatively insensitive to the $T_m^0(\infty)$ value used in the analysis. It will emerge later that the Regime II→III transition is not only where the effective substrate length reaches an irreducible value but is also where steady-state reptation begins to give way to the reptation of slack in the crystallization process.

Practically coincident with our first mention of Regime III[10,12], Phillips[14] made a proposal along somewhat different lines concerning the existence of such a Regime. While the present treatment is considerably more complete, Phillips suggested correctly that strip completion was unimportant so that $G_{III} \propto i$, and recognized further that the number of adjacent stems was small.

REGIME III KINETICS

In Regimes I and II, by far the largest number of stems laid down that contribute to growth in the G direction are a result of the substrate completion process that takes place at a velocity g. In Regime III, where the effective substrate length is highly restricted because of the abundance of niches, we postulate that crystallization is accomplished to a considerable degree by primary nucleation of stems on the surface. Thus, we expect the observable growth rate G_{III} to be proportional to $i' \propto \exp[-4b_0\sigma\sigma_e/(\Delta f)kT]$.

More formally we may write for the overall observable growth rate

$$G_{III} = b_0 i' L' = b_0 i' n_s' a_0 \tag{9}$$

where b_0 is the relevant layer thickness, a_0 the width of a stem, i' the nucleation rate in nuclei·s^{-1}·cm^{-1}, and n_s' is the mean (small and roughly constant) number of stems that are laid down in the 'niche' adjacent to the newly nucleated stem. The quantity L' in $L' = n_s' a_0$ may be thought of as an 'effective' substrate length. We take n_s' to be roughly 2 to 4 (see later), and independent of the overall substrate length L.

The calculation of i' is straightforward, and we give here a simplified version of its derivation. The general formula for the nucleation rate is[2]

$$i' = S_T/n_s a_0 = \frac{1}{a_0 n_s l_u} \int_{2\sigma_e/(\Delta f)}^{\infty} S(l)\mathrm{d}l \tag{10}$$

where $S(l)$ is the flux as a function of l and the fundamental rate constants to be noted below, S_T the total flux, and l_u the length of a monomer unit. The usual formula[1] $S(l) = N_0\mathbf{A}_0(\mathbf{A}-\mathbf{B})/(\mathbf{A}-\mathbf{B}+\mathbf{B}_1)$, while applicable to and derived specifically for the case where a large number of stems add to a nucleus forming a long substrate run, is not admissible here. In deriving the form of $S(l)$ just mentioned, the explicit assumption was made that ν, the number of stems (nucleus + stems in substrate), was large. In the present case we need only consider a few stems, and select three such stems ($n_s' = 3$) for purposes of illustration. The model is shown in *Figure 3*. The third stem added completes the substrate on a local basis, which means the rate constant $\mathbf{B}_c \cong 0$. It is readily shown (*cf.* Frank and Tosi)[15] that this leads to

$$S(l) = N_0\mathbf{A}_0\left\{\frac{1}{1+\mathbf{B}_1/\mathbf{A}+\mathbf{B}_1\mathbf{B}/\mathbf{A}_c\mathbf{A}}\right\} \tag{11}$$

where N_0 is the effective occupation number of the ground (subcooled liquid) state, and

$$\mathbf{A}_0 = \beta_g e^{-2b_0\sigma l/kT} \tag{12a}$$

$$\mathbf{B}_1 = \beta_g e^{-a_0 b_0 l/(\Delta f)kT} \tag{12b}$$

$$\mathbf{A} = \beta_g e^{-2a_0 b_0\sigma_e/kT} = \beta_g e^{-q/kT} \cong \mathbf{A}_c \tag{12c}$$

$$\mathbf{B} = \beta_g e^{-a_0 b_0 l/(\Delta f)kT} \tag{12d}$$

Equations (12) refer to the simple case $\psi = 0$. (The

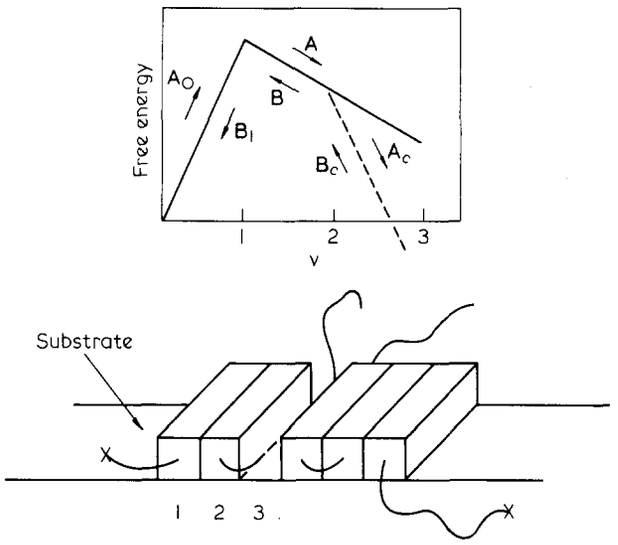

Figure 3 Model for Regime III growth (schematic). The particular model shown corresponds to $n_s' = 3$. The symbol ν represents the number of stems. $\mathbf{A_0}, \mathbf{B_1}, \mathbf{A}, \mathbf{B}$, etc., are the elementary process rate constants given by equation (12)

formulae corresponding to equation (12) for $\psi \neq 0$ are given in ref. 2.) Low values of ψ are readily justified[2]. Anticipating that $\mathbf{A} > \mathbf{B}_1$ and $\mathbf{A}_c\mathbf{A} > \mathbf{B}_1\mathbf{B}$ we have to this approximation

$$S(l) \cong N_0 \mathbf{A}_0 = N_0 \beta_g e^{-2b_0\sigma l/kT} \tag{13}$$

(It can be shown that $\mathbf{B}_1/\mathbf{A} \cong \exp[-a_0(\Delta f)/\sigma]$ and that $\mathbf{B}_1\mathbf{B}/\mathbf{A}_c\mathbf{A} \cong \exp[-2a_0(\Delta f)/\sigma]$. At $\Delta T = 26°C$ one then gets for PE the results $\mathbf{B}_1\mathbf{A} \cong 0.57$ and $\mathbf{B}_1\mathbf{B}/\mathbf{A}_c\mathbf{A} = 0.32$, which gives the factor in brackets in equation (11) as 0.53.) The term $2b_0\sigma l$ is the work required to put down an isolated single stem with two exposed lateral surfaces. A result similar to equation (13) is obtained for models related to that shown in *Figure 3* including those where the effective substrate is somewhat longer or shorter.

On a provisional basis we utilize β_g as given by equation (3c) to represent the retardation in the melt. This expression implies the applicability of the steady-state reptation process involving much or all of the pendant chain characteristic of Regimes I and II. (Recall that in the steady-state process, the overall friction coefficient is proportional to the length of the pendant chain, which is the physical basis for the factor $1/n$ in β_g.)[2] It will emerge subsequently that this is reasonable just at the inception of Regime III, but requires modification to account for 'slack' or 'stored length' at lower temperatures. Finally, recalling that N_0 is equal to $(\bar{z}\, n_s)\,(C_n P_0)$ according to equation (4b), we have with the mean value theorem applied to $\bar{z}$

$$i' = S_T/n_s a_0 = \frac{\beta_g N_0}{a_0 n_s l_u} \int_{2\sigma_e/(\Delta f)}^{\infty} e^{-2b_0\sigma l/kT} \mathrm{d}l$$
$$= (N_0 \beta_g p_i / a_0 n_s) e^{-4b_0\sigma\sigma_e/(\Delta f)/kT} \tag{14}$$

Observe that i' turns out under the approximations noted to be identical to i as given in equation (3a). Thus the surface nucleation rate in nuclei·cm^{-1}·s^{-1} is given by the same expression in Regimes I, II, and III.

Combining equations (9) and (14) gives the growth rate in Regime III as

$$G_{\mathrm{III}} = (C_{\mathrm{III}}/n) e^{-Q_D^*/RT} e^{-K_{g(\mathrm{III})}/T(\Delta T)} \tag{15a}$$

where

$$C_{\mathrm{III}} = \kappa\, p_i (C_n P_0)(kT/h) b_0 \bar{z} n_s' \tag{15b}$$

and

$$K_{g(\mathrm{III})} = 4b_0\sigma\sigma_e T_m^\circ/(\Delta h_f)k. \tag{15c}$$

It can be seen from equation (15a) that the slope of a plot of $\log_{10}G + Q_D^*/2.303RT$ [or $\log_{10}G + U^*/R(T - T_\infty)$] against $1/T(\Delta T)$] in Regime III is twice that of a similar plot for Regime II, but the same as that of Regime I. Thus $K_{g(\mathrm{III})} = K_{g(\mathrm{I})} = 2K_{g(\mathrm{II})}$. Notice that g is not involved in the expressions for G_{III}.

Regime III and Regime I have identical nucleation exponents, but there is a large difference in these Regimes in the pre-exponential factors:

$$G_{0(\mathrm{I})}/G_{0(\mathrm{III})} = (C_{\mathrm{I}}/n)/(C_{\mathrm{III}}/n) = n_s/n_s' \sim n_s/3 \tag{16}$$

The difference between $G_{0(\mathrm{I})}$ and $G_{0(\mathrm{III})}$ is substantial. For example, in the case of PE, the substrate length is ~ 0.11 μm^2 so that $n_s \cong 2.42 \times 10^2$, which suggests $G_{0(\mathrm{I})}/G_{0(\mathrm{III})} \sim 80$.*

For completeness we give the initial stem length l_g^* for Regime III. This is calculated as

$$l_g^* = \frac{1}{l_u} \int_{2\sigma_e/(\Delta f)}^{\infty} l S(l)\mathrm{d}l \Big/ \frac{1}{l_u} \int_{2\sigma_e/(\Delta f)}^{\infty} S(l)\mathrm{d}l \tag{17}$$

which with the approximate form for $S(l)$ given in equation (13) comes to

$$l_g^* = 2\sigma_e/(\Delta f) + kT/2b_0\sigma \tag{18}$$

A more detailed analysis[1,2] changes the second term (often denoted 'δl') to $kT/b_0\sigma$, but the difference is of trivial importance in the present case.

Equation (18) is for all practical purposes identical to that which obtains for Regimes I and II. Thus we may expect that the system will not abandon the mostly chain-folded lamellar habit as it enters Regime III, and it is further to be anticipated that the initial lamellar thickness l_g^* will quite generally fall with lowering crystallization temperature irrespective of whether crystallization occurs in Regimes I, II, or III. Some changes in gross crystal morphology may occur near the II→III transition owing to the rapid onset of the very rough growth front characteristic of Regime III (see later). We would remark that the true value of the initial stem length or fold period l_g^* is most apt to be found experimentally at quite low crystallization temperatures in Regime III, since here secondary processes such as a rapid but limited initial thickening during substrate completion prior to the addition of a new layer will be minimized or eliminated. The rapid though limited initial thickening we envisage here that might occur during strip completion on the actual growth front is to be distinguished from the slower and commonly observed isothermal thickening process wherein the body of the crystal increases its overall thickness.

* Note added in proof: C. M. Guttman and E. A. DiMarzio have recently completed a detailed Monte Carlo study of the 'bricklayer' problem that reproduces in detail the rate behaviour of Regimes I, II and III.

We now note a point of considerable theoretical interest. It is not necessary to invoke fluctuation treatments of stem addition to understand in at least broad aspect the tendency of the lamellar thickness to retain a value centring about l_g^* during substrate completion and growth in Regime III. The small cluster size and high nucleation rate in Regime III is such that *the fold period l_g^* is rapidly and continuously re-established every three or so stems* as the chain-folded clusters are put down on the substrate. One thus has reasonable assurance for this Regime that the fold period (before secondary processes such as isothermal thickening take place) will remain close to l_g^* during the lamellar growth process. The fluctuation treatments of substrate completion of Frank and Tosi[15] and Lauritzen and Passaglia[16] provide a convincing explanation of the persistence of the lamellar thickness at a value centring narrowly around l_g^* at higher crystallization temperatures corresponding to Regime I and Regime II where the substrate runs are long (see pp. 592–597 of ref. 1 for a discussion of the theories of fluctuation of fold period during substrate completion). Accordingly, one has a theoretical justification for the persistence of the lamellar thickness (prior to isothermal thickening) at a value centring about l_g^* for all three Regimes; no 'δl' or 'l_g' catastrophe occurs in PE with the fluctuation treatments in Regimes I and II for *any* value[1] of ψ, and the present treatment of Regime III prevents the 'l_g^* catastrophe' for allowable values of ψ down to very low crystallization temperatures.

PREDICTIONS AND APPLICATIONS

Polyethylene

The overall picture of Regime III crystallization in its kinetic manifestation, including its relationship to Regimes I and II, can best be delineated by calculation of plots of $\log_{10}G$ against ΔT and $\log_{10}G+Q_D^*/2.303RT$ against $1/T(\Delta T)$. This has the advantage of providing a direct guide for experimentation. Below we carry out the task for PE fractions. The Regime II→Regime III transition is accompanied by readily recognizable kinetic effects.

In previous work on nine PE fractions ranging from $M_z=2.65\times10^4$ to 2.04×10^5 that clearly exhibited the Regime I→Regime II transition it was found experimentally assuming $T_m^\circ(\infty)=145^\circ$C that[2]

$$C_{\rm I}=5.00\times10^{13}\ {\rm cm\,s^{-1}} \tag{19}$$

and

$$C_{\rm II}=3.34\times10^{7}\ {\rm cm\,s^{-1}} \tag{20}$$

under the condition that $K_{g(\rm I)}=2K_{g(\rm II)}$ where $K_{g(\rm I)}$ was found to be $1.800\times10^5\ {\rm K^2}$. The calculated absolute growth rate for each fraction falls close to the experimental value over a range of ΔT when these values are used with equations (6) and (7)[2]. (This accords with the theory for the pre-exponential factors with $\kappa\cong8.67$ which is well within expectation[2].) $K_{g(\rm I)}$ is calculated from $\sigma_e=90$ erg cm^{-2}, $\sigma=11.2$ erg cm^{-2} $b_0=4.55\times10^{-8}$ and $\Delta h_f=2.8\times10^9$ erg cm^{-3} (10^7 erg = 1 J) to be 1.800×10^5 K^2, which is in good accord with the mean experimental value[2] of 1.857×10^5 K^2 when the Regime I data are analysed without applying the condition $K_{g(\rm I)}=2K_{g(\rm II)}$. Now according to Regime I and Regime II theory, the slope of both $G(T)$ against ΔT and $\log_{10}G+Q_D^*/RT$ *versus* $1/T(\Delta T)$ should fall off as Regime II is entered, the latter plot by a factor of two. Thus $K_{g(\rm II)}$ should be close to 0.900×10^5 K^2; the mean experimental value is in fact 0.900×10^5 K^2 as obtained from plots of $\log_{10}G+7000/2.303\ RT$ against $1/T(\Delta T)$ for Regime II for the 9 specimens studied[2]. Hence, one can be quite certain of the Regime I and Regime II theories in this application.

Accordingly, for PE we have for Regimes I and II the expressions

$$G_{\rm I}=\left(\frac{5.00\times10^{13}}{n_z}\right)e^{-7000/RT}e^{-1.800\times10^5/T(\Delta T)} \tag{21}$$

for $\Delta T\leqslant16^\circ$C, and

$$G_{\rm II}=\left(\frac{3.34\times10^{7}}{n_z}\right)e^{-7000/RT}e^{-0.900\times10^5/T(\Delta T)} \tag{22}$$

for $\sim23^\circ{\rm C}\geqslant\Delta T\geqslant16^\circ$C. Recall from equation (7c) that $C_{\rm I}=5\times10^{13}$ in equation (21) contains the factor n_s, which is known to be 242 for the input data given here[2]. This value of n_s corresponds to $L=n_sa_0=1.1\times10^{-5}$ cm $=0.11$ μm.

It is a simple matter to make an estimate of the growth rate for Regime III with the help of equations (15). Here one uses the known constants[2] for Regimes I and II, namely $\kappa=8.67$, $p_i=4.59$, $b_0=4.15\times10^{-8}$ cm, $\bar z=150$ together with the estimate that $n_s'\cong3$ to get $C_{\rm III}=6.20\times10^{11}$ cm s^{-1}. This procedure is equivalent to multiplying $C_{\rm I}$ by the ratio $n_s'/n_s=3/242$. Thus, we find for Regime III the provisional estimate

$$G_{\rm III}\cong\left(\frac{6.20\times10^{11}}{n_z}\right)e^{-7000/RT}e^{-1.800\times10^5/T(\Delta T)} \tag{23a}$$

applicable at $\Delta T\geqslant\sim23^\circ$C. (In all of the above expressions we have taken $T_m^\circ(\infty)$ to be 145°C.) An analysis shows that $G_{\rm II}=G_{\rm III}$ at $\Delta T=23.2^\circ$C, which is generally similar to the conclusion drawn from the calculation of S_n depicted in *Figure 2*. It should be understood that equation (23a) is provisional in the sense that the β_g implicit in this expression may at temperatures below the Regime II→Regime III transition require modification since here only the slack may participate in the crystallization process.

In anticipation of the possibility that mostly only the 'slack' portions of the chain may crystallize at low temperatures in Regime III, and recalling that the effective activation energy function at low crystallization temperatures in a number of polymers is of the form[1,2,17] $\exp[-U^*/R(T-T_\infty)]$ rather than $\exp(-E_D^*/RT)$, one can construct the following equation for Regime III:

$$G_{\rm III}^*\cong\left(\frac{4.04\times10^{9}}{n^*}\right)e^{-1500/R(T-201)}e^{-1.800\times10^5/T(\Delta T)}. \tag{23b}$$

In obtaining this second provisional estimate, we have employed the standard values[1,17] $U^*=1500$ cal mol^{-1}, $T_\infty\cong T_g-30^\circ$C, and arranged the pre-exponential constant so that $G_{\rm III}^*=G_{\rm III}=G_{\rm II}$ at $\Delta T=23.2^\circ$C. (In calculating T_∞, we have used the value of $T_g=231$ K given by Davis and Eby[18]; see footnote 19 for discussion.) In the case of

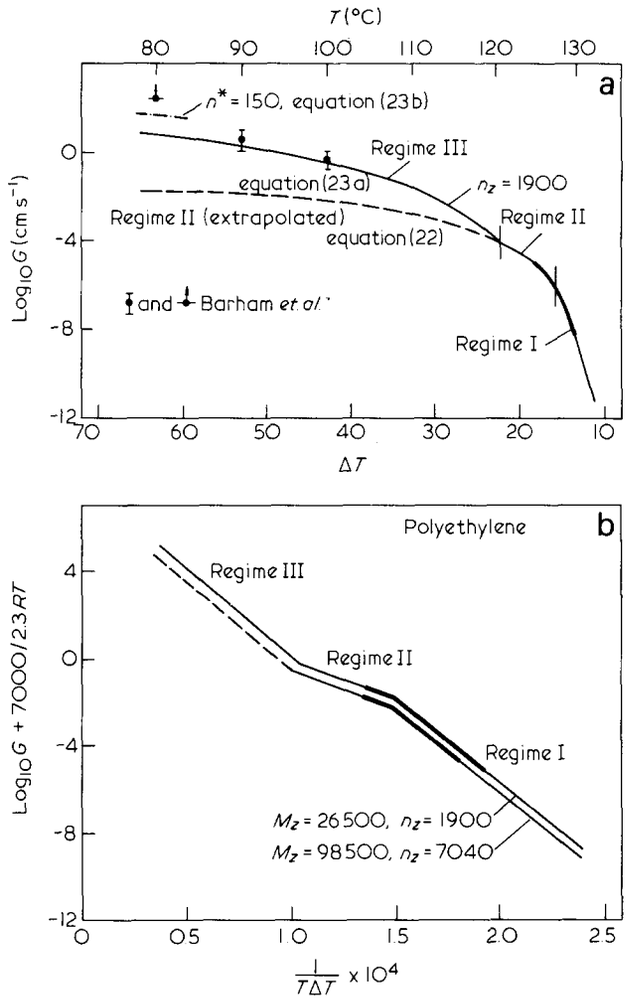

Figure 4 Calculated growth rate for polyethylene fractions in Regimes I, II, and III. (a) Solid lines represent plot of $\log_{10} G$ *versus* T and ΔT for fraction with n_z = 1900 for Regimes I, II, and III according to equations (21–23) and calculated using $T_m^0(\infty)$ = 145°C, and T_m^0 corrected at 143°C to account for finite molecular weight. Data points at 80°, 90° and 100°C due to Barham *et al.*[6,21]. Broken line shows fictive values of growth rate resulting from incorrect extrapolation of Regime II to low temperatures. Heavy solid line shows where isothermal growth rate has been measured experimentally in Regimes I and II (refs. 2 and 3). (b) Solid lines give plot of $\log_{10} G$ + 7000/2.3 RT *versus* $1/T(\Delta T)$ according to eqs. (21–23a). G is in cm s^{-1}. Heavy solid lines show where growth rate has been measured experimentally in Regimes I and II (refs. 2 and 3)

equation (23b), n^* may be considered as the effective slack length. This point will subsequently be discussed further. The above treatment implies that β_g as expressed in equation (3c) is replaced by $\beta_g^* = (\kappa^*/n^*)(kT/h) \exp[-U^*/R(T-T_\infty)]$. Note that this formulation emends C_{III}/n in equation (15a) to read $\kappa^* p_i (C_n P_0)(kT/h) b_0 \bar{z} n_s'/n^*$ and replaces $\exp(-Q_D^*/RT)$ with $\exp[-U^*/R(T-T_\infty)]$ in the same equation, thus converting G_{III} to G_{III}^*.

Figure 4 shows plots of $\log_{10} G + 7000/2.303\ RT$ *versus* $1/T(\Delta T)$ for two PE fractions, one with $M_z = 26\,500$, $n_z = 1900$, and the other with $M_z = 98\,500$, $n_z = 7040$ calculated using equations (21–23a). Also shown is a plot of $\log_{10} G$ *versus* T and ΔT for the fraction of lower molecular weight. (Between $\Delta T = 23.2$°C and $\Delta T \cong 140$°C equations (23a) for G_{III} and (23b) for G_{III}^* give quite similar results for a given n or n^*, but at considerably larger ΔT, corresponding to crystallization temperatures below 275 K, equation (23b) gives progressively smaller values of the growth rate in Regime III, and leads to cessation of growth at T_∞. The range where growth rate data[2,3] are known for these fractions in Regimes I and II is shown in each case as a heavy solid line.) A more detailed representation of the fit between theory and experiment for Regimes I and II is given in reference 2.

The plots in *Figure 4* show the overall behaviour of Regimes I, II and III. The growth rates in Regime III at large undercoolings are far greater than would be predicted at the same undercooling with Regime II theory. Also shown is a curve (-·-·-) calculated for temperatures near 80°C ($\Delta T \cong 64$°C) using equation (23b) for G_{III}^* with $n^* = 150$. This value of n^* is based on a rough estimate of the entanglement distance in PE obtained from melt viscosity data (see later).

No great accuracy is claimed for the Regime III growth rate calculations, but they do serve to show the general nature of the rate phenomena that attend the onset of Regime III, and may be regarded as a reasonable guide for experimental investigations. The chief characteristic is a break *upward* in the slope of the rate of crystallization as Regime III is entered from Regime II. This is just the opposite of what happens to the rate as Regime II is entered from Regime I, where there is a *downward* break.

For reasons to be indicated shortly, it is of interest to calculate G_{III} and G_{III}^* at 80°C, which for samples of moderate molecular weight, corresponds to $\Delta T \cong 64$°C if $T_m^\circ(\infty)$ is taken as 145°C. With equation (23a) one finds G_{III} (80°C) = 5.2 cm s^{-1} for $n_z = 1900$ and with equation (23b) one gets G_{III}^* (80°C) = 3.9 cm s^{-1} for $n^* = n_z = 1900$. Further, if one assumes provisionally with equation (23b) that $n^* \cong 150$ refers to the number of chain units associated with the slack length, which is sufficient to allow at least two adjacent stems to enter the substrate for the l_g^* relevant to 80°C, then G_{III}^* (80°C) comes to ~68 cm s^{-1}. These are very large rates, and are all far greater than the value $G_{II} \cong 1.5 \times 10^{-2}$ cm s^{-1} for $n_z = 1900$ than one would estimate by (incorrectly) using equation (22) on the assumption that Regime II type growth prevailed at 80°C in PE. (The value $G_{III}^* \sim 68$ cm s^{-1} is toward the upper limit of what we deem reasonable for expressions derived on the basis noted[20].) Below we shall quote evidence suggesting that Regime III theory provides a reasonable representation of what is known about the growth rate of PE at low crystallization temperatures.

No experimental observations of the growth rate of PE fractions near the predicted Regime II→Regime III transition appear to be available. However, there are firm indications from the work of Barham *et al.*[6] that Regime III theory is appropriate at low crystallization temperatures in PE. Specifically, these authors have found the following growth rates for subcooled PE droplets *circa* 2 to 3 μm in diameter: $G \geqslant 200$ cm s^{-1} at 80°C[6], $G \cong 3.5$ cm s^{-1} at 90°C, and $G \cong 0.55$ cm s^{-1} at 100°C. The latter two measurements[21] were on an NBS fraction $M_w = 32\,000$ or $n_w = 2290$, and are correct to within better than a factor of three. These data are plotted in *Figure 4a.*

It is evident from *Figure 4* that Regime III theory provides a considerably better explanation of the observed growth rates at low temperatures than does Regime II. The expression for G_{III}, i.e., equation (23a), appears to be adequate at 90° and 100°C, while G_{III}^* as given by equation (23b) appears best at 80°C. Accordingly, these results stand in general support of the existence of Regime III crystallization in PE.

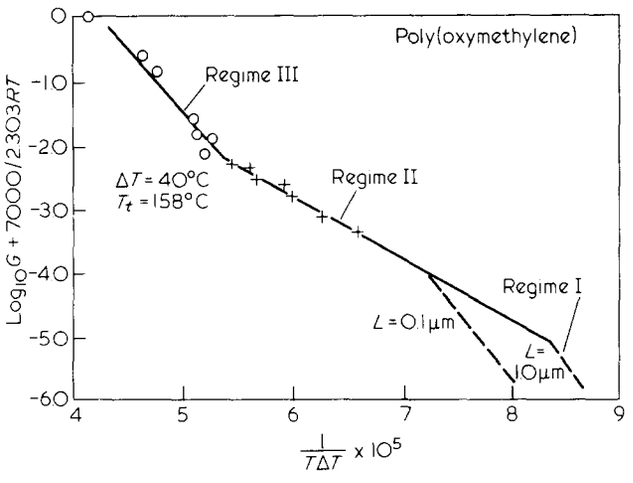

Figure 5 Plot of $\log_{10} G + Q_D^*/2.3\,RT$ against $1/T(\Delta T)$ for poly(oxymethylene) in Regimes II and III. Solid lines calculated according to equations (24) and (25). G is in cm s^{-1}. The data points in Regimes II and III are derived from the work of Pelzbauer and Galeski[5]. Note upward break as Regime III is entered (compare with *Figure 4b*). Regime I behaviour calculated according to equation (28)

We would remark here that we could have carried out the analysis on PE using any value of $T_m^\circ(\infty)$ between about 142°C and 146°C without incurring any major change in physical interpretation. As was shown earlier for Regimes I and II[2], such quantities as $K_{g(I)}$ and $K_{g(II)}$ and the concommitant values of σ, κ and P_0, would have been lower for a lower $T_m^\circ(\infty)$, but the Regime III transition would have appeared at essentially the same absolute temperature, and the properties of Regime III exhibited in *Figure 4* would not be greatly altered.

Although the full experimental case for Regime III crystallization in PE is yet to be made, it is evident from the foregoing comparison of theory with experiment that confidence can be placed in the predictions in a general way. From a theoretical point of view, the niche separation calculation given earlier strongly suggests the existence of Regime III type crystallization. In the next section we shall show that the type of behaviour associated with the Regime II→Regime III transition has been seen in detail in POM.

Poly(oxymethylene)

A clear case can be made for the existence of a Regime II→Regime III transition in melt-crystallized POM. The particular material to be discussed is Delrin 150, which is a 'capped' linear polymer with $M_n \sim 70\,000$. In their studies of the rate of crystal growth of this material, which refers to the stable and high melting common hexagonal form, Pelzbauer and Galeski[5] noticed a break in the spherulite radial growth rate data similar in all major respects to that predicted in *Figure 4* for PE in the Regime II→Regime III region. They represented their data for POM as describing two straight lines on a plot of log $G + U^*/R(T - T_\infty)$ against $1/T(\Delta T)$ that intersect at 158°C, which corresponds to an undercooling of about 40°C. They used values of U^* and T_∞ corresponding to the Williams–Landel–Ferry (WLF)[22] equation. It is easily deduced from their paper that the change of slope is not far from two, as required by the theory outlined here for the Regime II→III transition. We have regenerated the original data points from various plots in their paper, and replotted these in *Figure 5* as $\log_{10} G$ (cm s^{-1}) + 7000/2.303 RT against $1/T(\Delta T)$. In making this analysis we have assumed that the activation energy Q_D^* for reptation is the same for POM as for PE. The melting point $T_m^\circ = 471.5\,K = 198.3°C$ given by Pelzbauer and Galeski was used in the analysis. Rybnikar[23] obtained this value from a T_m' *versus* T_x plot for the hexagonal form, and found the slightly higher value $T_m^\circ = 475.7\,K = 202.5°C$ for the same form from a T_m' *versus* $1/l$ plot. Amano, Fischer and Hinrichsen[24] state that the experimentally observed melting point of extended-chain POM is close to 200°C. The results and conclusions given below are relatively insensitive to changes in T_m° in the range just noted, and also do not depend critically on the value assumed for Q_D^* (or U^* and T_x).

It is readily seen by a comparison of *Figures 4* and *5* that the general features predicted for Regime III are met. In quantitative terms, we find from the data of Pelzbauer and Galeski the following expressions for POM:

$$G_{III}(\text{cm s}^{-1}) = 2.83 \times 10^8\, e^{-7000/RT} e^{-4.576 \times 10^5/T(\Delta T)} \quad (24)$$

and

$$G_{II}(\text{cm s}^{-1}) = 1.63 \times 10^3\, e^{-7000/RT} e^{-2.308 \times 10^5/T(\Delta T)} \quad (25)$$

These expressions intersect at 158°C or $\Delta T \cong 40$°C.

Notice that

$$K_{g(III)}/K_{g(II)} = 4.576 \times 10^5/2.308 \times 10^5 = 1.983 \quad (26)$$

which is only about one per cent lower than the theoretical value of 2. This certainly lies well within the experimental error of the K_g values, which is about 9 per cent. We have also examined the $K_{g(II)}$ and $K_{g(III)}$ values obtained from plots of $\log_{10} G + U^*/2.303R(T - T_\infty)$ *versus* $1/T(\Delta T)$ with $U^* = 1500$ kcal mol^{-1} and $T_\infty = T_g - 30°C$, and find nearly the same K_g values as quoted above. Thus, the analysis is not particularly sensitive to the choices of the type of plot used, and we may draw the conclusion that the upswing in $G(T)$ at 158°C corresponds closely to the characteristics predicted for the Regime II→III transition.

Another check is possible which further confirms the above conclusion. The ratio of the pre-exponential factors is readily shown to be

$$G_{0(III)}/G_{0(II)} = (p_i/2f)^{\frac{1}{2}} (C_n P_0)^{\frac{1}{2}} \bar{z}^{\frac{1}{2}} n_s' e^{q/2kT}. \quad (27a)$$

With $C_n P_0 = 100$, $(p_i/2f)^{\frac{1}{2}} = 2$ as for PE, and $\bar{z} = 100$, $n_s' = 3$, and $q = 9000$ cal mol^{-1} (see later) we estimate

$$G_{0(III)}/G_{0(II)} \sim 1.2 \times 10^5 \text{ (theory)}. \quad (27b)$$

From equations (24) and (25) the experimental value is seen to be

$$G_{0(III)}/G_{0(II)} = (2.83 \times 10^8)/(1.63 \times 10^3) = 1.74 \times 10^5 \text{ (experiment)}. \quad (27c)$$

The main properties of Regime II and Regime III, and the transition between them, seem satisfied in the case of Pelzbauer and Galeski's data on POM. We conclude that their low temperature data represent an authentic in-

stance of the Regime III behaviour that has been predicted.

It is a simple matter to estimate for POM using the values of $K_{g(II)}$ and $K_{g(III)}$ that $\sigma\sigma_e$ is 2700 erg^2 cm^{-4} and 2680 erg^2 cm^{-4} respectively in Regimes II and III. Using $\sigma = 0.1\ (ab)^{\frac{1}{2}}\ \Delta h_f$ with $a_0 b_0 = 17.15 \times 10^{-16}$ cm^2 and $\Delta h_f = 3.55 \times 10^9$ erg cm^{-3}, we estimate $\sigma = 14.7$ erg cm^{-2}, $\sigma_e = 183$ erg cm^{-2}, and $q = 2a_0 b_0 \sigma_e = 6.28 \times 10^{-13}$ erg/fold = 9000 cal mol^{-1} of folds. Both Regimes II and III give essentially these results, so there is no major change in fold surface free energy between Regimes II and III. This 'kinetic' value of σ_e is in fair accord with the independent thermodynamic determination $\sigma_e \cong 205$ erg cm^{-2} found by Rybnikar[23] from a T_m' *versus* $1/l$ plot. If his T_m' *versus* $1/l$ data are adjusted to the T_m° of 198.3°C, then $\sigma_e \cong 171$ erg cm^{-2}. Accordingly we see no major discrepancy in our analysis. We observe also that Pelzbauer and Galeski quote $\sigma_e = 183$ erg cm^{-2} for the region we have recognized as Regime III.

It is possible to give a rough estimate of the temperature where the Regime I→Regime II transition might be found in POM. This will occur at the temperature or undercooling where G_{II} is equal to G_I. To generage an estimate of G_I it is only necessary to multiply G_{III} by the ratio n_s/n_s'. For the case $n_s = 280$, which corresponds to a substrate width $L \cong 0.1$ μm, we find with $n_s' = 3$ that

$$G_I\,(\text{cm s}^{-1}) \sim 2.6 \times 10^{10}\, e^{-7000/RT} e^{-4.576 \times 10^5/T(\Delta T)}. \quad (28)$$

It is then found that the Regime I→II transition occurs at $\Delta T = \sim 32$°C or $T_x \cong 166$°C. This estimate depends critically on the estimate of n_s (or L) and the use of $L = 1$ μm would put the Regime I→Regime II transition at $\Delta T \sim 27$°C or $T_x = 171$°C where the growth rate would be so slow as to require an investigation of great duration ($G_I \sim 2.5 \times 10^{-10}$ cm s^{-1} or ~ 0.22 μm/day at $\Delta T = 27$°C).

It is of interest to compare the experimental results for PE and POM in the light of the analysis given. The experimental values of the pre-exponential factor $G_{0(II)} = C_{II}/n$ do not differ greatly. For POM for which $n \cong 4000$, $G_{0(II)}$ is $\sim 1.63 \times 10^3$ cm s^{-1} and that for PE is $(3.34 \times 10^7)/(4 \times 10^3)$ or 8.35×10^3 cm s^{-1} at the same n. The principal cause of the much lower growth rates at a given ΔT in hexagonal POM as compared with PE is thus not in the pre-exponential factors, but rather in the considerably larger work of chain folding q for this polymer ($q_{PE} \sim 4900$ cal mol^{-1}; $q_{POM} \sim 9000$ cal mol^{-1})[25]. Through the relation $\sigma_e = q/2a_0 b_0$, this is the main factor that caused $K_{g(II)}$ and $K_{g(III)}$ in equations (7) and (15) to be much larger for POM than PE, which has a very strong effect on reducing $G(T)$ at a given ΔT. The fact that the I→II and II→III Regime transitions are predicted to occur at larger ΔT values in POM than in PE can be traced to the same basic cause.

We must now ask why q is so much larger for POM than PE. This can be understood beginning with the fact that the *trans–gauche* energy difference is larger for POM (~ 1500 cal mol^{-1})[26] than it is for PE (~ 600 cal mol^{-1}). Then assuming roughly the same number of twisted bonds per fold in both polymers, it is reasonable that $q_{POM} \sim 2\ q_{PE}$, which is seen from the kinetic analysis given above to be the case.

We complete the analysis of POM by remarking on the kinetically determined stem length as calculated from equation (18). (The corresponding calculation for PE has been given elsewhere.[1]) Using the values of T_m° *and* Δh_f already quoted for POM, together with the value of $\sigma_e = 183$ erg cm^{-2} determined from kinetics, we estimate that the initial stem length l_g^* is approximately

$$l_g^*(\text{Å}) = 4860/(\Delta T) + 4.7. \quad (29)$$

At $T_x = 150$°C ($\Delta T = 48.3$°C), which is in Regime III, this gives

$$l_g^*\,(\text{theoretical}) = 105\ \text{Å}, \quad (30)$$

and at $T_x = 167$°C ($\Delta T = 31.3$°C), which is in Regime II, it yields

$$l_g^*\,(\text{theoretical}) = 160\ \text{Å}. \quad (31)$$

The more exact form of equation (18) with the second term given as $kT/b_0\sigma$ simply adds 4.7 Å to each result (1 nm = 10 Å).

Rybnikar[23] has measured the low-angle X-ray spacings of Delrin 150 POM at these temperatures and found them to be ~ 240 Å ($T_x = 150$°C) and ~ 340 Å ($T_x = 167$°C). As in the corresponding case of PE, these specimens had undoubtedly undergone isothermal thickening during crystallization, and by careful melting point measurements Rybnikar found that such thickening had in fact occurred by a factor of $\gamma \cong 2.5$ in Delrin 150 POM. In cases where there exists no large angle of tilt, it is reasonable to compare the theoretical estimates given in equations (30) and (31) above with the initial lamellar thickness l_g^*(experimental) calculated from Rybnikar's X-ray data as follows:

At $T_x = 150$°C,

$$l_g^*(\text{experimental}) \cong 240/2.5 = 96\ \text{Å} \quad (32)$$

and at $T_x = 167$°C

$$l_g^*(\text{experimental}) \cong 340/2.5 = 136\ \text{Å}. \quad (33)$$

It can be seen from the above that the experimental estimates of the initial lamellar thickness are approximately consistent with the l_g^* calculated with the kinetically determined value of σ_e. Accordingly, there is no reason to suspect that the kinetically determined value of σ_e is grossly incorrect in either Regimes II or III. A somewhat better analysis of the variation of the initial lamellar thickness with crystallization temperature can be obtained by permitting the fold surface free energy to depend slightly on temperature and take the form $\sigma_e = \sigma_{e0}[1 + y(\Delta T)]$ where y is a small positive number *circa* ~ 0.01 to 0.02[1]. This tends to reduce the variation of l_g^* with temperature somewhat, though the overall trend and magnitude is similar to the simpler case with constant σ_e treated here. Recall also that it is this small temperature dependence of σ_e that is one cause of C_2 in $l_g^* = 2\sigma_e/(\Delta f) + C_2$ appearing to be larger than δl[1]. The rapid though limited initial thickening that may occur during substrate completion prior to the addition of a new layer that was mentioned earlier could also contribute to C_2.

The analysis of the crystallization rate data and lamellar thickness data of POM given here that involves

Regime III removes some apparent anomalies that had appeared in the application of the kinetic nucleation theory of chain folding. In particular, the failure of a plot of log $G+U^*/R(T-T_\infty)$ *versus* $1/T(\Delta T)$ for Rybnikar's POM data to be fit by one straight line is convincingly explained by the presence of the Regime II→Regime III transition (see *Figure 5*). At the same time, the advent of Regime III theory renders it possible to avoid the postulate forced on Pelzbauer and Galeski by the absence of such a theory that the hexagonal form of POM exhibited two types of fold, one with almost exactly twice the fold surface free energy as the other. As noted earlier, an appropriate use of Regime II and Regime III theory leads to the same fold surface free energy in Regimes II and III, which is a more satisfactory situation in view of the fact that only one crystal form (hexagonal) is involved.

MOLECULAR MORPHOLOGY IN REGIME III: THE VARIABLE CLUSTER MODEL

General considerations and constraints

Considerable information can be deduced from the kinetic model for Regime III concerning the arrangement of the molecules in the crystalline lamellae, especially when it is understood that there exist definite limitations on the probability of non-adjacent re-entry resulting from the necessity of avoiding a density paradox at the lamellar surface. Such an anomaly can result from an excessive number of non-adjacent loops or interlamellar links. In the following discussion we shall note the fact that the Regime III model definitely predicts the existence of amorphous material (non-adjacent re-entrant random-coil loops) that is largely associated with the lamellar surface. As noted earlier, the discussion assumes some relevance in connection with the interpretation of small angle neutron scattering (SANS) experiments on quench-crystallized PEH–PED mixtures.

Consider now the situation depicted schematically in *Figure 6* (upper diagram) where a molecule is being put down between two previously formed surface patches denoted J and K where the niche separation is $S_n=4a_0$. This niche separation is chosen as being reasonably representative on the basis of the kinetic considerations discussed earlier (see discussion following equation (8)). As the molecule begins substrate completion at patch J, it is confronted with two energetically favourable proximate sites (niches) for re-entry, first at (i), which represents an adjacent re-entry and also at (ii) which is a non-adjacent re-entry with an intervening random-coil loop. The particular path we have depicted is (ii). Because of the proximity of the adjacent niche, event (i) is perhaps more probable than (ii), but the latter must still be considered. Event (ii) clearly illustrates the origin of non-adjacent re-entry on a kinetic basis: the niches are by a considerable margin the most probable sites for re-entry, since there is a *gain* in stability of $a_0b_0\,\delta l(\Delta f)$ in so doing[1,10], and when the niches are close together, non-adjacent re-entry is a definite possibility. (If a stem goes down on the substrate without an adjacent niche a *decrease* in stability of $l_g^*[2b_0\sigma - a_0b_0(\Delta f)]$ is incurred[10], showing that such events are disfavoured during substrate completion compared to attachment at a niche.) From the foregoing it might seem that the limiting case for Regime III might be mostly non-adjacent re-entry (i.e. a 'switchboard' model) or, alternatively, the situation shown in *Figure 6a* between surface patches K and M, which is a fringed micellar structure. As will be discussed below, neither of these is correct on any large scale, provided that the stems are not very strongly tilted with respect to the fold plane.

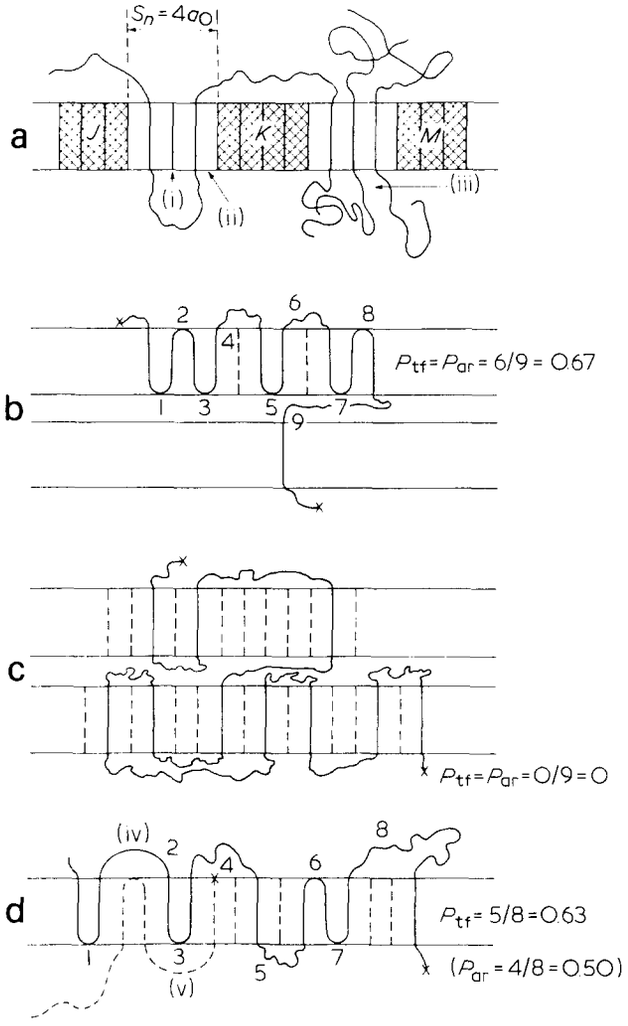

Figure 6 Allowed and forbidden molecular morphologies in substrate formation: variable cluster model (schematic). (a) Symbols *J*, *K*, and *M* represent pre-existing surface patches with niches on each edge. Left diagram shows allowed non-adjacent re-entry at a niche at (ii). Right diagram shows disfavoured fringed micellar structure at (iii) that violates Gambler's Ruin treatment on local basis. (b) Simplified variable cluster model illustrating calculation of p_{ar} and p_{nar} (allowed Model). (c) Simplified random re-entry switchboard (forbidden model). (d) Variable cluster model illustrating 'leap frog' type tight fold at (iv). Tilt not shown

We now inquire into the limitations that exist concerning the amount of non-adjacent re-entry that can be tolerated in a lamellar system. This inquiry will also provide much information on the amount of adjacency. Following our previous work[10,27], we begin by defining an 'index' or 'descriptor' for the degree of adjacency and non-adjacency. To accomplish this, we imagine that a given molecule has a trajectory as it enters the growth front as a stem, then adds new adjacent stems with intervening chain folds for a time on that front, and finally emerges and wanders at random in the amorphous phase to another point on the same or a different lamella where it re-enters the crystal. This process is repeated until the molecule is in place in the semicrystalline system. In this process, *an adjacent re-entry is called a 'successful try', and a non-adjacent re-entry is called a 'failure'*. We then define

the descriptor for the degree of adjacent re-entry, which is simply the probability for adjacent re-entry, as

$$p_{ar} = \frac{\text{number of successful tries (adjacent re-entries)}}{\text{total number of tries}} \tag{34}$$

The corresponding descriptor for the degree of non-adjacent re-entry, which is just the probability for non-adjacent re-entry, is

$$p_{nar} = 1 - p_{ar} = \frac{\text{number of failures (non-adjacent re-entries)}}{\text{total number of tries}} \tag{35}$$

If $p_{ar} = 1$, i.e., $p_{nar} = 0$, the lamella is completely regularly chain-folded (except for chain end effects), and if $p_{ar} = 0$ ($p_{nar} = 1$), the lamella is a random switchboard with no adjacency whatsoever.

The descriptors p_{ar} and $p_{nar} = 1 - p_{ar}$ are important because it is through them that the degree of adjacency and non-adjacency can be quantified for a model that is proposed for the molecular morphology, and because the Gambler's Ruin treatment places definite bounds on the upper limit for p_{nar} and thence the lower limit of p_{ar}. By the use of these descriptors and their known limits as derived from the Gambler's Ruin treatment, it is thus possible to distinguish between possible and forbidden models for the molecular morphology. Other information must of course be introduced to further refine the possible set of models.

We illustrate the calculation of p_{ar} and p_{nar} for a model by selecting a simple case where special types of structures with 'tight' but longer than normal folds, or 'tight' folds that represent nearest-neighbour jumps to a contiguous lattice plane, do not occur. Then we are restricted to situations of the type shown in *Figure 6b*, where only strictly adjacent re-entry in a specified lattice plane, and non-adjacent re-entries in the same plane, or a different lamella, occur. The arrangement shown is a simple form of the variable cluster model. The calculation of p_{ar} for this molecular morphology is illustrated in *Figure 6b*. Tries 1, 2, 3, 5, 7 and 8 are 'successful', the sum being 6, and the total number of tries is 9. Therefore for the molecule shown in *Figure 6b*, which is in the variable cluster morphology, we have

$$p_{ar} = 6 \text{ successes}/9 \text{ tries} = 2/3 \tag{36a}$$

and

$$p_{nar} = 3 \text{ failures}/9 \text{ tries} = 1/3 \tag{36b}$$

The three 'failures' are at 4, 6 and 9. It is understood that the loops between non-adjacent re-entries in *Figure 6a* and *6b* represent random flight liquid-like configurations.

It is instructive to introduce yet another example. Consider the model shown in *Figure 6c*. The sample molecule has the same overall length as that depicted in *Figure 6b*, and also has ten stems in the two lamellae. However, there are no adjacent re-entries. As before, the loops between non-adjacent re-entries and the interlamellar link are random flights. Therefore for the molecule shown in *Figure 6c*, which is a simplified form of the 'random switchboard' model, one has

$$p_{ar} = 0 \text{ successes}/9 \text{ tries} = 0 \tag{37a}$$

and

$$p_{nar} = 9 \text{ failures}/9 \text{ tries} = 1. \tag{37b}$$

Values of p_{ar} and p_{nar} very similar to those given above will be found for any random switchboard model. We shall now examine the limits that exist for p_{ar} and p_{nar}.

It has long been realized that p_{nar} had an upper bound that was far below unity. For example, Frank[28] in 1958 gave an argument that was equivalent to the statement $p_{nar} \leqslant \sim 0.5$. This approximate estimate has recently been discussed and reviewed by Frank[29]. More recently, Guttman *et al.*[4] have given a treatment of the issue using the mathematics associated with the 'Gambler's Ruin' problem which shows that if the random-coil amorphous phase associated with long loops and interlamellar links is to have a normal liquid density that

$$p_{ar} \geqslant \sim 2/3 \tag{38}$$

and

$$p_{nar} \leqslant \sim 1/3. \tag{39}$$

In terms of the models depicted in *Figures 6b* and *6c*, it is seen that the Gambler's Ruin treatment forbids the class of model generally called the 'random switchboard' (*Figure 6c* and equations (37)) but allows models of the general type depicted in *Figure 6b* where equations (36) give p_{ar} and p_{nar} values that are acceptable. Subsequently we shall by various means provide more detail concerning the variable cluster model, and show further that it appears naturally as the dominant molecular morphology in Regime III.

The physical reason for the upper bound of p_{nar} of $\sim 1/3$, and the corresponding lower bound on p_{ar} of $\sim 2/3$, is readily discerned both from Frank's arguments and the Gambler's Ruin treatment[4]. If p_{nar} exceeded $\sim 1/3$, the surface amorphous zone would contain too many segments and have an excessively high local density. If a random coil entity emerged from every surface site, the amorphous phase near the lamellar surface would exhibit a density nearly three times larger than that of the normal liquid[4]. This type of density paradox was first clearly demonstrated for a switchboard type model by Guttman *et al.*[30] (see also reference 10) by a computer simulation procedure prior to the formulation of the Gambler's Ruin treatment. Specifically, the modified random switchboard ('$p_{es} = 0.3$') model of Yoon and Flory[31], which contained virtually no adjacent re-entry by hypothesis, i.e., $p_{ar} \equiv \sim 0$ and $p_{nar} \equiv \sim 1$, was found to exhibit an amorphous surface zone of considerable thickness which had a density about twice that of either the crystal or the normal subcooled liquid.

With the advent of the Gambler's Ruin treatment, one has a formal rationale for rejecting all models with approximately vertical stems (see below) which have a p_{nar} much in excess of 1/3. Accordingly, models where each of the molecules in the lamellae behave statistically like that shown in *Figure 6c* must be rejected. Equations (38) through (41) greatly lower the probability that substrate growth involving the insertion of consecutive isolated chains giving a local fringed micelle such as shown in *Figure 6a* at (iii) will occur in large numbers. Thus the Gambler's Ruin treatment provides a firm basis for understanding why 'strange' molecules, i.e., new mo-

lecules that consecutively form a set of contiguous stems, each with random coils at either end, can enter the growth front only in limited numbers. Such 'pinned' random coils possess a high segment density close to the surface, and crowding them together clearly leads to an inadmissably high local density in the amorphous surface zone.

The calculations leading to equations (38) through (41) are based on the assumption that the chain axes in the crystal are perpendicular to the lamellar surface[4]. A very large departure from the perpendicular ($>70°$) is required to allow p_{nar} to approach unity[4,29]. There is no evidence that linear PE and POM exhibit such a large tilt, so we may expect equations (38)–(41) to hold at least approximately for these polymers.

If special structures involving longer than strictly nearest-neighbour adjacent 'tight' folds, or adjacent-type jumps to a contiguous lattice plane involving 'tight' folds are allowed, then the restrictions given by equations (38) and (39) are revised so that the probability of 'regular' or 'tight' folding is[4]*

$$p_{tf} \geqslant \sim 2/3 \tag{40}$$

and the probability of non-adjacent re-entry with an intervening random-coil type loop is

$$p_{nar} \leqslant \sim 1/3. \tag{41}$$

One (not necessarily common) type of 'tight' or 'regular' fold that is covered by this more general set of restrictions is illustrated in *Figure 6d*. The molecule represented as a solid line has 'regular' or 'tight' folds which are not random coils at (iv) and (v). Ordinary adjacent re-entry folds are also 'regular' or 'tight' folds. The molecule in *Figure 6d* is seen to have $p_{tf}=5/8=0.625$, $p_{ar}=4/8=0.50$, and $p_{nar}=3/8=0.375$.

As defined here, a strictly adjacent re-entry refers to stems that are nearest neighbours in a given lattice plane in which the intervening chain fold is short enough so that it does not have random-coil character. Accordingly, the fold is not a 'loose' loop. *All 'tight' folds have the property that they do not contribute to the amorphous phase, and the site of re-entry is very close to that of emergence.* 'Tight' or 'regular' folds are those in the following categories[4,32]: (1) as previously noted ordinary adjacent re-entry folds are classified as 'tight' folds; (2) folds that execute a short straight-line non-random coil transit to a second or third nearest neighbour in a specified lattice plane are classified as 'tight' folds; and (3) a fold that makes a short straight line non-random coil excursion to a nearest neighbour in a contiguous lattice plane is a 'tight' fold. The latter definition of a lattice plane change 'tight' chain fold would include a short non-random coil fold at a jog between two lattice planes, such as the short fold that might connect the stems at the intersection of the 110 and 200 planes in PE. Later, in discussing neutron scattering data we shall at times refer to such a 'lattice plane change fold' as being involved in 'fold surface roughening'[32]. We would not count a long random-coil loop connecting two adjacent stems from the same molecule as a chain fold. Almost all the known data, including those from neutron scattering (see later), can be dealt with using only adjacent re-entry folds and lattice plane change chain folds, i.e., types (1) and (3) above.

Special structures such as those shown at (iv) in *Figure 6* have been suggested by Sadler ('leapfrog' model)[33]. These are 'tight' folds by definition (2) above. When the situation on both sides of the lamella is considered, it would appear that one way they could occur is to occassionally allow molecules to go down on the substrate pairwise for short distances. We do not expect this to be particularly common. The special structures referred to here are discussed in more detail elsewhere[32].

It is readily seen that the limitation on the upper bound of p_{nar} noted by Frank[28,29], or the more precise limitations expressed in equations (38)–(41), prevent virtually unlimited non-adjacent re-entry such as is implied by the random switchboard model. In the simplest case described above (equations (38) and (39), and *Figure 6b*) the niches in the substrate completion process must on the average be filled by an act of adjacent re-entry about two times out of three. In the more general case (equations (40) and (41)), 'tight' or 'regular' folds must occur about two times out of three: such 'regular' folds may be either normal adjacent re-entry, a tight 'leapfrog' structure, or an adjacent-type jump to a contiguous lattice plane such as may occur at a jog. On balance, we consider that perhaps the commonest type of tight fold (other than strictly adjacent re-entry) will be an adjacent-type 'tight' transit to a contiguous lattice plane, with either the same or different indices. When the latter structures are present, the probability of simple adjacent re-entry can fall below $p_{ar}\sim 2/3$, but we consider that it is unlikely to fall much below 0.4 to 0.5; p_{tf} will in such cases still retain a value near 2/3. It is only when equations (40)–(41) are obeyed that an inadmissably high density can be avoided in the amorphous phase at the lamellar interface[4].

Guttman *et al.*[4] have examined the possibility that liquid state orientation effects near the lamellar surface could alter equations (38)–(41). It was concluded that these bounds were not seriously affected by such orientation, except in one case where the lower bound for p_{tf} was actually increased above 2/3. Thus, surface amorphous zone orientation does not appear to be a panacea that allows one to evade the fact that the lamellar surface consists mostly of tight folds, provided that the stems are at least approximately vertical.†

As an aside, the author wishes to urge that when a model for the molecular morphology of a semicrystalline lamellar polymer is proposed that the values of p_{tf} or p_{ar} and p_{nar} be cited, together with any information on the angle of tilt of the stems. If this were done, it would be a simple matter to determine whether or not the model was a possible one.

With the aforementioned constraints on the degree of non-adjacent re-entry with intervening 'amorphous' or random-coil type loops, it is possible to construct a picture of a number of aspects of the molecular morphology characteristic of Regime III that is also consistent with findings based on the kinetics.

* The exact formula, derivable from ref. 4, for the cubic lattice case is

$$p_{tf} \geqslant 1-(\rho_a/\rho_c)(1/3\cos\theta)$$

where θ = angle of tilt as measured from the vertical and ρ_a/ρ_c = ratio of amorphous to crystal density. Slightly lower p_{tf} values are found with the rotational isomeric model.

† It is emphasized that the Gambler's Ruin treatment does not preclude the presence of a thin (*circa* ~10 Å) somewhat oriented amorphous zone contiguous to the fold surface boundary.

Origin of the variable cluster model

In this section, we shall discuss the origin of the variable cluster model characteristic of Regime III crystallization as it is generated in a kinetic process that has certain conditions imposed on it by the Gambler's Ruin calculation that essentially limits the amount of non-adjacent re-entry. The treatment will allow estimates to be made of the number of stems n_s' of width a_0 that comprise the effective substrate length $L' = n_s' a_a$, these estimates being independent of the kinetics. It is apparent that the value of n_s' is important in understanding and quantifying Regime III behaviour.

Earlier, we have given analyses of the rate data concerning PE and POM that utilized the assumption that $n_s' \sim 3$. The concept that n_s' is fairly close to this value, say from 2 to 4, was derived from intuitive arguments connected with the niche separation calculation for PE illustrated in *Figure 2*. While the aforementioned calculations with $n_s' \sim 3$ was satisfactory, it can hardly be claimed that n_s' has actually been determined from the growth rate data.

It will be shown below that a fairly close estimate of n_s' can be deduced from neutron scattering measurements on quench-crystallized PEH–PED mixtures, which can be analyzed to obtain values of the mean non-adjacent re-entry 'loop' length, the mean straight line throw distance for such an amorphous loop, and the mean cluster size. (There is reasonable assurance that the quench-crystallized PEH–PED mixtures used in neutron scattering studies[7] were in fact of the Regime III type. The actual crystallization temperature of the PEH–PED specimens was estimated to be $119 \pm 3.5\,C$[31], which corresponds to $\Delta T \sim 26 \pm 3.5\,C$, which from *Figure 2* and equations (22) and (23a) suggests Regime III growth.) It will be shown further that the variable cluster model with $n_s' \sim 3$ is consistent with degree of crystallinity measurements on quench-crystallized PE samples. All these calculations are better understood after a brief discussion of the origin of the variable cluster model, including comments on those restrictions of non-adjacent re-entry that are imposed by the Gambler's Ruin treatment.

For convenience we shall assume at the outset that the mean value of the substrate length is about $3a_0$, corresponding to $n_s' \sim 3$. This means that the average run or mean effective substrate length where adjacent stems can be laid down on the substrate in a given crystal plane is of about this size. (The stems in a run need not all represent adjacent re-entries.) Meanwhile it must be realized that these runs will not all be the same length, because the initiating stems are put down at random positions on the substrate. Accordingly, some substrate completion runs will be longer than 3 or 4 stems, while others will be shorter. Some will be single stems. An isolated stem can arise, for instance, when a portion of a molecule is trapped in a double niche as shown in the lower diagram of *Figure 3*. A set of adjacent stems is termed a 'cluster'. Each cluster must be formed in the kinetic process of putting down the stems in a substrate run. Remembering that if each substrate run contains an average of roughly 3 stems, we must expect the average cluster to be about this size, or slightly smaller. Because the effective substrate length varies about its mean value, one must expect the cluster size also to vary about its mean. Hence the term 'variable cluster' model.

The upper bound on the mean cluster size is associated with kinetic considerations above the Regime II→Regime III transition, since here the niche separation becomes large (see expressions for S_k and N_k and *Figure 2*). *The lower bound on the mean cluster size is at all temperatures determined by the Gambler's Ruin constraints.* Application of these constraints insures that no abnormally high density builds up at the lamellar surface. The mean minimum cluster size $\langle v_c \rangle_{min}$ for a molecule of high molecular weight with vertical stems is given by[4]

$$\langle v_c \rangle_{min} = 1/p_{nar} \cong 3 \tag{42}$$

The value of $\langle v_c \rangle_{min}$ is somewhat less than three for a chain of finite molecular weight. This argument immediately places a lower bound on the mean length of a substrate run of $\sim 3a_0$, i.e., $n_s' \sim 3$, in Regime III. Throughout Regime III, the mean effective substrate length will be close to this lower bound because the niche separation will strive to be as small as possible.

The foregoing leads readily to a pictorial 'sample' representation of the variable cluster model characteristic of Regime III. This is depicted for the particular case where the clusters are confined to a single lamella in *Figures 7a, 7b* and *7c*, since this elucidates most of the features characteristic of the model in a simple manner. The top three diagrams in *Figure 7* refer to different representations of the morphology of the same molecule. The number of stems in the crystal is 16, which allows the possibility of a total of 15 'tries' for adjacent re-entry. If the molecule were PE with a lamellar thickness of 160 Å, the representation would refer to a specimen of $M \sim 43\,000$, including the segments in the random-coil loops which will represent about one-third of the chain.

Figure 7a is a diagram of essentially the conventional type, which shows however that the molecule can change lattice planes. One of the lattice plane changes involves a non-adjacent re-entry, while the other involves a tight fold. There are 16 stems in 7 clusters, so the mean cluster size is 16/7 or ~2.3. (This is slightly smaller than the observed cluster size of 2.7 to 3 to be noted later, but the model is still generally illustrative.) The value of p_{tf} is 10/15 or 0.67, $p_{ar} = 9/15$ or 0.60, and p_{nar} is 5/15 or 0.33 in accord with equations (40) and (41). The non-adjacent re-entries are taken to be random coils, and the clusters are randomly placed within the confines of the two planes.*

Figure 7b shows the trajectory of the same molecule with the 7 clusters denoted 1, 2, ... 7 in a three-dimensional view designed to highlight the 'skyscraper' outline of the rough growth front resulting from the intense multiple nucleation that occurs in Regime III. It will be recalled that the rough growth front and the variable cluster size is consistent with the kinetic processes described earlier for Regime III. Some stems from other molecules are shown, but without details of the molecular conformation. When crystallization is completed these molecules must in the end have approximately the same

* Note that we have counted the stem in position 6 in *Figure 7b* as a single stem cluster in finding the number of clusters to be seven, even though a short fold of normal length connects this stem to cluster 5. (See also *Figure 7c*). This approach lowers $\langle v_c \rangle$ from $16/6 \cong 2.7$ to $16/7 \cong 2.3$, and requires that the aforementioned lattice plane change fold between clusters 5 and 6 be classified as a 'tight' fold contributing to p_{tf}, but not as a typical adjacent re-entry fold contributing to p_{ar}. This calculation of $\langle v_c \rangle$ may imply too stringent a definition in some applications; the most appropriate definition of a 'cluster' depends on the experimental technique used to measure $\langle v_c \rangle$.

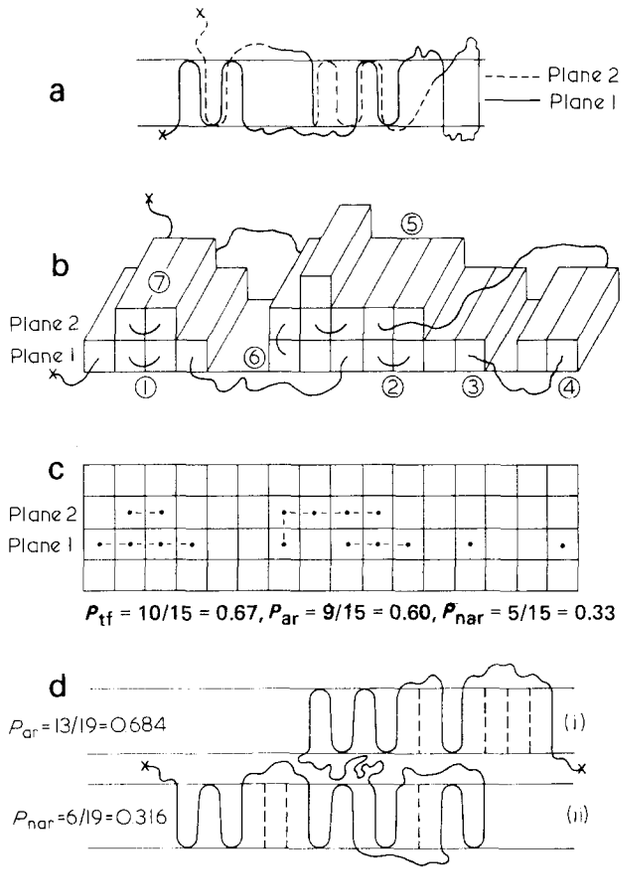

Figure 7 Variable cluster model for Regime III crystallization (schematic). a, b and c are different representations of same molecule in variable cluster conformation. Note rough growth front depicted in b. Diagram d illustrates variable cluster model with interlamellar link between lamella (i) and lamella (ii). These models apply near inception of Regime III. At lower crystallization temperatures, the 'paired stem' version of the variable cluster model is probably more appropriate. Models have been simplified somewhat by deliberate omission of 'leapfrog' conformation of type shown in *Figure 6d*. All models depicted here conform to requirements of Gambler's Ruin treatment, and show a probability of non-adjacent re-entry of 1/3 or less. Tilt not shown

average values of p_{tf}, p_{ar}, p_{nar}, and $\langle \nu_c \rangle$ as the sample molecule depicted.

The 'trajectory' of any specified molecule, such as that labelled 1, 2, ... 7 in *Figure 7*, while useful in defining a final 'sample' conformation in the crystal, does not necessarily represent the actual sequence in which the clusters were laid down. In the variable cluster model, segments from many different molecules are reeled onto a given section of the rough growth front forming small substrates averaging $n_s' \sim 3$ stems, and any nearby molecule may fill such a substrate with a cluster so long as the Gambler's Ruin conditions are not violated. It is therefore a simple matter to see that the small clusters may not go down strictly in the 'trajectory' sequence. It is also seen that by the same mechanism they will end up in the crystal with a liquid-like overall conformation (see later), while still exhibiting two-thirds tight folds. The formation of the lamellar crystal is not a result of a sort of 'nucleative collapse' of the subcooled liquid state involving no more than a simple straightening of a set of segments to form isolated stems, but instead involves some reptation to allow sets of chain-folded clusters each averaging about three stems to be put down on the growth front. Certain details of this reptation process will be discussed later in this work.

Figure 7c illustrates again for the same molecule the arrangement of the stems in the lattice as viewed end-on. Here one readily sees the three isolated stems corresponding to clusters 3, 4, and 6 in *Figure 7b*. One also readily observes four other clusters, one of two stems 7, one of three stems 2, and two with four stems, 1 and 5.

For the sake of completeness, *Figure 7d* shows a molecule with 20 stems, corresponding to $M \sim 54\,000$ for PE, that exhibits an interlamellar link between lamellae (i) and (ii). This molecule has $p_{ar} = 13/19 = 0.684$, $p_{nar} = 1/19 = 0.316$, and $\langle \nu_c \rangle = 2.86$.

As will be seen later, the $\langle \nu_c \rangle$ value just given is typical of that found for quench-crystallized PEH–PED samples by neutron scattering studies[30,32]. Though they undoubtedly exist, lattice plane change tight folds have not been depicted in *Figure 7d* in order to avoid undue complication of the diagram. A molecule can participate in two or more lamellae, depending on its length. Neutron scattering analyses clearly show that the number of interlamellar links in quench-crystallized PE is restricted to about 0.5 to 1.0 per molecule when the molecule consists of 2500 to 3500 $-CH_2-$ units[30,32]. This comes to roughly one interlamellar link for each 10 to 20 surface sites.*

The diagrams given in *Figure 7* have been simplified to the extent that we have not invoked special 'tight' folds of the type shown at (iv) and (v) in *Figure 6d*. This may occur to some extent[32,33], but many of the main features of the variable cluster model can be dealt with without this complication. Recall that these structures, together with lattice plane change folds, can reduce the degree of strictly adjacent re-entry even though p_{tf} is about 2/3.

While it must be remembered that the diagrams in *Figure 7* are only 'sample' representations, and that they are of a schematic character, they still have value in that they depict a number of important aspects of the molecular morphology of PE when crystallized near the inception of Regime III. This is particularly true with regard to the mean cluster size, and the rather high probability of tight folding. The significance of these points will become apparent after the discussion to follow concerning neutron scattering data on PEH–PED mixtures.

One important consequence of the Gambler's Ruin treatment is that exactly one-third of the mass of the amorphous phase between the crystalline lamellae will consist of chain units in the interlamellar links; the other two-thirds of the amorphous phase will be comprised of chain units that are non-adjacent re-entry loops that emerge from and re-enter the same lamella[4]. We shall use this fact later in estimating the degree of crystallinity associated with the variable cluster model for Regime III.

From the arguments given earlier it was found for the variable cluster model that

$$\frac{1}{p_{nar}} \cong \langle \nu_c \rangle_{min} \sim n_s' \tag{43}$$

Analysis of neutron scattering data on quench-

* The Gambler's Ruin treatment specifies the fraction of surface sites occupied by interlammellar links, f_{link}, as the reciprocal of the number of statistical steps corresponding to the thickness of the amorphous zone, l_a[4]. For $l_a = 90$ Å, $f_{link} \cong 1/10$.

crystallized PEH–PED mixtures using a number of models, for example, the 'central core'[30,32] and 'variable cluster'[30,32,34] models persist in giving $\langle v_c \rangle$ values of 2.7 to 3[35] when the calculated radius of gyration and crystallinity are close to the experimental ones. Thus from equation (43) we deduce that our earlier use of $n_s' \sim 3$ in the analysis of kinetic data appears to be justified.

The aforementioned neutron scattering analyses also yield the mean straight line throw distance for a non-adjacent re-entry in the same lamella. A 'random coil' type amorphous chain with $\langle x \rangle$ chain units in its contour length connects the two stems. We denote that straight line distance between the separated stems as S_{ns}. We must expect S_{ns} to be comparable to $a_0 n_s'$. More formally, we may write

$$S_{ns} \cong a_0(n_s' - 1). \tag{44}$$

The neutron scattering analyses for the central core and variable cluster models quite generally give values of S_{ns} of *circa* 22 Å[30,32,34] for quench-crystallized PEH–PED. With a_0 taken to be 4.55 Å, equation (44) then gives $n_s' = 3.8$, which is in satisfactory agreement with the determination given previously. Somewhat smaller values of n_s' are found if lattice planes other than 110 with larger a_0 are assumed (see later).

We conclude from the SANS studies on PEH–PED that n_s' is very probably in the range of about 2.5 to 4, and accordingly believe that the values $n_s' \sim 3$ or $n_s' \sim 4$ used at various places in the kinetic analyses were good approximations.

In explaining the detailed origin of the degree of crystallinity associated with Regime III crystallization, it will prove useful to know the average number of chain units in a non-adjacent re-entry loop. While this can be estimated closely by Monte Carlo methods using 'real chain' statistics for the random coil excursions in the amorphous state, there exists a simple general formula for this number, which we denote $\langle x \rangle_{\text{loop}}$, that according to the Gambler's Ruin problem comes to[4]

$$\langle x \rangle_{\text{loop}} = 2l_a/d, \tag{45}$$

where l_a is the thickness of the amorphous phase between the crystalline lamellae, and d the bond length, which is 1.54 Å for PE. Notice that the mean loop length depends on the interlamellar spacing l_a. From a physical standpoint, this occurs because a greater interlamellar distance allows a longer excursion in the amorphous phase before the chain terminates, even if that termination is on the same lamella from which it originated. For PE, where l_a is typically taken as 90 Å for quench-crystallized material[30–32], the contour length of the loop is 180 Å, and the number of $-CH_2-$ units in the average-sized loop is $\langle x \rangle_{\text{loop}} = 117$. Recall that the mean straight-line distance between the point of emergence and termination of a loop between non-adjacent re-entries on a given lamella is *circa* 22 Å for PE.

Radius of gyration of the variable cluster model

Some important properties of the variable cluster model will now be noted. We begin with remarks on the radius of gyration.

Monte Carlo calculations carried out by Guttman[34] show that *a molecule with the variable cluster morphology exhibits a radius of gyration R_g that is practically identical to that of a random coil molecule in the melt, and further, has an R_g that varies as $M^{\frac{1}{2}}$. This occurs despite the rather high degree of regular folding because of the small size of the clusters, the distribution in the size of the clusters, and the random placement of these clusters.* SANS experiments on quench-crystallized PEH–PED mixtures (which must have been crystallized close to or in Regime III) have shown[7] that $R_g \propto M^{\frac{1}{2}}$, and little change of R_g on crystallization. This was at first interpreted to mean that random re-entry (i.e. 'switchboarding' with $p_{ar} \sim 0$) was by far the most probable event during crystallization[31]. In view of the discussion given earlier, and a recent detailed study[32], it is clear that the variable cluster model with its high degree of regular or adjacent folding and concommitant absence of a density anomaly presents a considerably more likely explanation of the SANS data on melt-crystallized PEH–PED mixtures of moderate molecular weight than the alternative just noted.

In summary, the variable cluster model has properties such that a rather high degree of adjacent or regular folding occurs together with a liquid-like radius of gyration. The implication to be found in the literature that these two properties are inconsistent and cannot occur together is erroneous.

Degree of crystallinity for variable cluster model

It is instructive to calculate the degree of crystallinity associated with the variable cluster model for quench-crystallized PE. We have specifically in mind the degree of crystallinity near the Regime II→Regime III transition, i.e., near $\Delta T \cong 23°$ where the concept of 'slack' does not have to be invoked (see later).

It was noted earlier for quench-crystallized PE that the mean number of chain units in a loop is $\langle x \rangle_{\text{loop}} = 117$ for an amorphous phase that is 90 Å thick. Further, from the Gambler's Ruin treatment[4], we know that we must account for the amorphous interlamellar links by multiplying $\langle x \rangle$ by 3/2. Now on the average, each loop is associated with a cluster of $\langle v_c \rangle$ stems, each of which has a length l_g^*, giving the number of $-CH_2-$ units in the crystalline cluster as $\langle v_c \rangle\, l_g^*/1.27$. Then with $l_g^* = 160$ Å and $\langle v_c \rangle = 2.7$, we find the mass fraction of amorphous component is

$$\varphi = 1 - \chi = \frac{\frac{3}{2}\langle x \rangle_{\text{loop}}}{\frac{3}{2}\langle x \rangle_{\text{loop}} + \langle v_c \rangle l_g^*/1.27} = 0.34 \tag{46}$$

i.e., the calculated degree of crystallinity is $\chi = 0.66$. The experimental value[7] observed for quench-crystallized PE at $\Delta T \sim 25°C$ is $\chi \cong 0.65$. Recalling that $\langle v_c \rangle \sim n_s'$, one can see that this calculation is not only consistent with the degree of crystallinity data, but also with the value of n_s' that has been suggested by other methods. Thus the surmise that $n_s' \sim 3$ in Regime III is consistent with the amount of amorphous component that occurs in Regime III at or near its inception in polyethylene. Of course φ is also equal (approximately) to $l_a/(l_a + l_g^*)$, where l_a and l_g^* are given at the outset, with the outcome that equation (46) is to be regarded as elucidating the detailed physical situation in the amorphous phase and the associated crystalline clusters, rather than being taken as an

a priori calculation of φ. A detailed theory for l_g^* is known[1], but no *a priori* calculation of l_a appears to be available.

The foregoing shows that the closely spaced niches given by Regime III theory, taken together with the restrictions imposed by the Gambler's Ruin treatment, lead in a natural way to an amorphous phase consisting of loops and an occasional interlamellar link that is associated with the otherwise chain folded lamellar surface.

Remarks on neutron scattering studies

It has already been noted that the Regime III variable cluster model predicts $R_g \propto M^{\frac{1}{2}}$ for a polymer crystallized in Regime III, where R_g for the semicrystalline state is very similar to that exhibited by molecules in the melt, and that this result is confirmed by SANS experiments in the low μ (Guinier) region on quench-crystallized PEH–PED mixtures. Below we summarize other information that has been deduced from SANS studies that is relevant to the molecular morphology of chain-folded systems formed at moderately large undercoolings that approximate the conditions of Regime III crystallization. This will allow us to further substantiate that the mean chain-folded cluster size in Regime III is about three.

Quench crystallization techniques must be used with PEH–PED mixtures to prevent isotopic segregation and isothermal thickening effects. Hence all current work on the molecular morphology associated with the crystalline phase of PE involves materials formed in or very near Regime III. With the R_g obtained from very low angle measurements being explained by the variable cluster model, we now inquire if the model can accommodate neutron scattering data at higher μ values in the range 0.01 to 0.14 ($\mu = (4\pi/\lambda)\sin(\theta/2)$).

Guttman *et al.* have shown in an extensive analysis[32] that two closely related forms of the variable cluster model can explain the overall SANS results on PEH–PED mixtures of a number of investigators. The basic problem is to (1) reproduce the observed scattering intensity at high μ with the model, at the same time obtaining (2) the correct liquid and crystal density and degree of crystallinity, and (3) the correct R_g value. It must be understood that the experimental agreement between various investigators with regard to absolute intensity of the relevant (i.e., coherent) scattering $\mu = 0.01$ to 0.14 from PEH–PED samples is not particularly good especially at larger μ (see *Figure 3* of reference 32 for a comparison of the data on PEH–PED mixtures of various investigators). Therefore one must still allow for some latitude in the interpretation.

One variable cluster type model that gave excellent results for PEH–PED involved putting some of the adjacent stems in the clusters on planes other than 110, and allowing for the roughness of the growth front by introducing lattice plane change chain folds. The SANS data were definitely consistent with a combination of surface roughening (i.e., with lattice plane change chain folds which are explicitly predicted by Regime III theory) and crystallization on a mixture of the 110, 200 and 310 growth planes (see *Figure 12* of reference 32). Basically, a part of what was done here to match the intensity at the higher μ values was to spread the stems somewhat further apart than they are on the 110 facet to reduce the predicted intensity: adjacent re-entry on the 200 and 310 facets accomplish this. The p_{ar} for this model (in which 'leapfrog' structures were not invoked) was close to 0.7. We regard this as a quite acceptable model. Roughening involving the 020 and certain other planes, was also considered.

Another way to fit the SANS data with the variable cluster model is to insert, in addition to a substantial fraction of normal adjacent stems, some special, i.e., 'leapfrog', type structures with 'tight' or 'regular' folds between once and twice removed stems on the 110 or 200 facet. This may be done either with or without surface roughening. Perhaps the best model of this type was one with surface roughening of the 110 and 200 growth planes for which $p_{nar} = 1/3$, $p_{ar} \cong 0.4$ and $p_{tf} = 2/3$ (see *Figure 17* of reference 32). As is seen in *Figure 7b*, the variable cluster model is definitely consistent with the concept of surface roughening. The reader is referred to the paper by Guttman *et al.*[32] for details of the molecular morphology consistent with the SANS studies.

Recent wide angle neutron scattering studies by Stamm[36], and Wignall, Mandelkern, Edwards, and Glotin[37], on quench-crystallized PEH–PED mixtures allow strictly adjacent re-entry with roughly 4 or so stems in the 200 and 020 planes (denoted by them as 100 and 010, respectively). Also, adjacent re-entry of about this number of stems in the 110 plane could not be ruled out. These results are in general consistent with the prior work of Guttman *et al.*, where it was shown that $\langle v_c \rangle \sim 3$ for PEH–PED[30,32,35]. Further, we consider these results to be consistent with the variable cluster chain morphology that we have proposed here on kinetic grounds (coupled with the Gambler's ruin limits) as that relevant to Regime III, and earlier as a model to explain the radius of gyration and scattering intensity observed in neutron scattering experiments[30,32,34]. The locally rough growth front and small cluster size in Regime III may in the end render it difficult to identify the dominant growth plane in quench-crystallized PE; as noted previously by Guttman *et al.*[32], a mixture of growth planes, such as 110, 200, 310, and 020 with runs of $n_s' \sim 3$ stems in each, seems to fit the facts known at present rather well.

Even though the precise details of the molecular morphology of quench-crystallized (i.e., Regime III crystallized) PE as revealed by neutron scattering are subject to some uncertainties, a number of essential points still stand out clearly: (1) the mean cluster size is about three; (2) the mean straight-line throw distance for a non-adjacent loop that emerges from and then re-enters the same lamella is ~ 22 Å; and (3) the radius of gyration is similar to that of the parent melt, and varies as $M^{\frac{1}{2}}$. *All of these items are individually consistent with the variable cluster model, and in sum, point directly to it. The kinetic picture we have presented, taken together with the Gambler's Ruin treatment, leads to the same model and yields the further point that the probability of 'tight' or 'regular' folding is close to two-thirds.*

Though it is in a sense an incidental issue in the present paper, it is worth noting what can occur when crystallization takes place at temperatures somewhat above the Regime II→Regime III transition. In this region, equations (40) and (41) still hold, but the effective substrate length is increased because the niches are further apart (see *Figure 2*). Then longer runs of stems with adjacent re-entry or regular folds are permitted, though not demanded. Thus, the variable cluster model can gradually give way with increasing crystallization temperature to the 'central core' model treated by Guttman *et al.*[10,30,32]

or the very similar 'ACA' type model of Guenet, Picot, and Benoit[38]. Here fairly long runs of adjacent stems may occur in a lamella, with random flight excusions to stems or sets of stems in the same or a different lamella, and R_g will vary as M^{α} where $\alpha > \frac{1}{2}$ ($\alpha \to 1$ for very long runs of adjacent stems). This latter point cannot be checked by SANS for PE because of isotopic segregation and isothermal thickening effects that occur at the higher crystallization temperatures. Fortunately, deuterated- and hydrogen-bearing isotactic polystyrene mixtures do not exhibit segregation, and it is highly significant that SANS studies with *i*–PSH–PSD mixtures of moderate molecular weight crystallized from the melt at a relatively high temperature are consistent with *long sheets of stems in the lamellae indicative of rather long runs involving adjacent re-entry in the* 330 *plane*[38] ('central core'[10,30] or 'ACA' type model[38]). Also, $R_g \propto M^{0.78}$ i.e., $\alpha > \frac{1}{2}$ in this case as expected. It is apparent from this example that one should not draw unduly general conclusions concerning the molecular morphology in *all* polymers from the restricted case of quench-crystallized PE, and that the kinetic theory can be a useful guide in understanding the differences in molecular morphology exhibited by a polymer crystallized at various temperatures. We would especially emphasize that the molecular morphology of a specified polymer will almost certainly depend to some extent on the crystallization temperature, with more regular folding with longer runs of adjacent stems being allowed, according to the kinetic theory, at the higher temperatures. Thus we anticipate that a given melt-crystallized polymer will not have one unique and fixed molecular morphology, but rather a gradation of fold surface perfection depending on the crystallization temperature.

Summary of molecular morphology for Regime III crystallization

Our overall conclusion is that the molecular morphology produced in Regime III crystallization near its inception for samples of normal molecular weight is in general similar to that illustrated in *Figure 7*. (A somewhat more detailed picture of the molecular conformation for the 'paired stem' version of the variable cluster model that may be characteristic of crystallization deep in Regime III will be given subsequently.) Certain details (such as growth on unusual lattice planes) are not shown, but the main features such as $p_{tf} \sim 2/3$ and $p_{nar} \sim 1/3$ and the mean cluster size $\langle \nu_c \rangle \sim 3$ are depicted in an approximately correct manner. Special attention is drawn to *Figure 7D* which illustrates an interlamellar link comprising about one-third of the total amorphous phase. This representation of the variable cluster model implies the correct crystallinity and radius of gyration, the total absence of a density anomaly at the lamellar surface, and is fully consistent with the small cluster size demanded by the small niche separation and rough growth front characteristic of Regime III. It is also consistent in the schematic sense in that the fraction of sites that are involved in interlamellar links is about one in ten rather than perhaps one in three as shown pictorially by Yoon and Flory[39,40]. Nothing in the physical properties of quench-crystallized PE of moderate molecular weight suggests such a high fraction of interlamellar links as roughly one in three. In any event, Backman and DeVries[41] have shown by e.s.r. measurements on fracture surfaces that the fraction of tie chains (interlamellar links) per crystal stem in PE is roughly one in 20, which is similar to the result of one in 10 to 20 found by SANS[10,32]. The Yoon–Flory representation, with its high fraction of interlamellar links, and with virtually no adjacent re-entry, has been criticized[4,10,32], particularly by Frank[29].

REPTATION AND CRYSTALLIZATION OF SLACK IN REGIME III

Reeling rate in Regime III with steady-state reptation

It has been demonstrated in earlier work[2] that steady-state reptation is rapid enough in Regime I and the upper part of Regime II in PE to allow the force of crystallization to pull a pendant chain onto the substrate at a rate sufficient to sustain considerable adjacent re-entry chain folding. In steady-state reptation, the overall friction coefficient resisting the 'reeling in' effect of the force of crystallization is proportional to the length of the pendant chain; this leads to the $1/n$ factor in β_g and thence to the prediction of a $1/M$ dependence of the growth rate in both Regimes. This is verified by experiment[2]. The best analysis implied that only a part of the pendant chain entered the growth strip with chain folding before an interruption (non-adjacent re-entry) occurred[2]. Thus, while the resistance felt by the force of crystallization involved the whole pendant chain in the time scale encountered in Regime I and the upper part of Regime II, it was not required that the whole chain enter without interruption. The reptation rates in these Regimes were such as to allow (though not demand) rather long runs of adjacent re-entry before an interruption. We shall now consider the case of Regime III.

Inasmuch as the surface nucleation rate i becomes very high in Regime III, we must inquire into whether the 'steady state' reptation rate in this Regime is sufficient to allow $n_s' \sim 3$ stems to be drawn onto the substrate with adjacent re-entry.

It is readily shown for Regime III that the reeling rate of a pendant molecule in cm s^{-1} that is demanded for the case of adjacent re-entry by the relationship between the nucleation rate i and the mean number of stems n_s' corresponding to the effective substrate length $L' = n_s' a_0$ is

$$r_{III} = i(n_s' l_g^*)(n_s' a_0) = i\, n_s'^2 a_0 l_g^*. \tag{47}$$

Now the steady state reeling rate characteristic of Regimes I and II, which involved movement under the force of crystallization $a_0 b_0 (\Delta f)$ of much of the pendant chain by steady-state reptation in a 'wormhole' consisting of its random-coil neighbours, is known from nucleation theory with reptation to be[2]

$$r_{nuc} = (l_g^*/a_0) g_{nuc} = (l_g^*/a_0) a_0 \left(\frac{\kappa}{n}\right) f \left(\frac{kT}{h}\right) e^{-Q_D/RT} e^{-q/kT} \tag{48}$$

for the case of $\psi = 0$, where g_{nuc} is as given in equations (4). (It is shown in ref. 2 that r_{nuc} as given by equation (48) is essentially equivalent to the reeling rate as calculated using the friction coefficient approach.) The number of stems that r_{nuc} can sustain with adjacent re-entry is given by setting r_{III} equal to r_{nuc} and solving for n_s'. This yields

$$n_{s_{lim}}' = \left(\frac{f}{p_i \bar{z} C_n P_0}\right)^{1/2} e^{-q/2kT} e^{K_{g(III)}/T(\Delta T)} \tag{49a}$$

for $\psi = 0$.

The theory for g_{nuc} can be carried out for ψ other than zero, and this leads $\exp(-q/kT)$ in equations (4a) and (48) to be replaced by $\exp[-q(1-\psi)/kT]$, where we expect $0 \leqslant \psi \leqslant \sim 1/3$. (See reference 2 for the relationship between ψ and the relevant rate constants **A** and **B**.) Recalling that q is the work of chain folding $q = 2a_0b_0\sigma_e$, it is seen that $\psi = 0$ implies that all the stems added to the substrate require chain folds; the case $\psi = 1/3$ implies that two out of three stems added involve chain folds, the remaining one being non-adjacent. Higher values of ψ than $\sim 1/3$ are thus forbidden, because the Gambler's Ruin treatment clearly excludes more than this fraction of non-adjacent stems ($p_{nar} \leqslant 1/3$).

With the above, the more general formula for $n'_{s\lim}$ is

$$n'_{s\lim} = \left(\frac{f}{p_i \bar{z} C_n P_0}\right)^{1/2} e^{-q(1-\psi)/2kT} e^{K_{g(II)}/T(\Delta T)} \qquad (49b)$$

The case $\psi = 1/3$ is probably the most realistic, and leads to slightly more rapid substrate completion than $\psi = 0$. For PE one has[2] $f = 0.615$ at $\Delta T = 23.2°C$, $p_i = 4.54$, $\bar{z} = 120$, $C_n P_0 = 100$, $q = 4900$ cal mol^{-1}, and $K_{g(II)} = 0.900 \times 10^5$ K^2. For a fraction where the molecular weight is such that T_m° is reduced below $T_m^\circ(\infty) = 145°C$ to $144°C = 417.2$ K, we find at the Regime II→ Regime III transition where $\Delta T = 23.2°C$, $T_x = 394$ K that

$$n'_{s\lim} \cong 2.8 \qquad (50a)$$

for $\psi = 0$, and

$$n'_{s\lim} \cong 7.9 \qquad (50b)$$

for the case $\psi = 1/3$.

The above calculations show that steady state reptation as given by equation (48), or its analogue with $\psi = 1/3$, is rapid enough at the inception of Regime III to allow $n'_s \sim 3$ *adjacent* stems to be put down between the niches. A calculation with equation (49b) with $\psi = 1/3$ shows that $n'_{s\lim} \sim 2$ at 117°C. This is essentially the absolute lower bound where steady-state reptation could be operative in Regime III and likewise represents a lower limit for the temperature of the Regime II→Regime III transition. Thus we see no basic objection to the approximate treatment leading to equations (15) and 23a) for G_{III} in Regime III for PE at the inception of Regime III. It is clear however from equations (50) that at undercoolings somewhat larger than 23.2°C that steady-state reptation, i.e., reptation where the friction coefficient is proportional to the length of the chain, will not of itself allow adjacent stems to participate in even the small clusters that form. It follows that some process other than steady-state reptation must at somewhat larger undercoolings allow segments to enter the growth front and rapidly form small clusters, since it is known that crystallization with folding takes place well into Regime III in PE.

Reeling of slack

There is clear evidence from the work of Barham *et al.*[6] that typical lamellar entities with some type of chain folding do in fact form in PE at much larger undercoolings than $\sim 23°C$. There is also evidence that the chains in these crystals are not strongly tilted with respect to the lamellar surface. (Recall that Barham *et al.* find this result in PE droplets crystallized at 80°C or $\Delta T \cong 64°C$.) Accordingly, we must ask what process might allow crystallization at such temperatures with an average

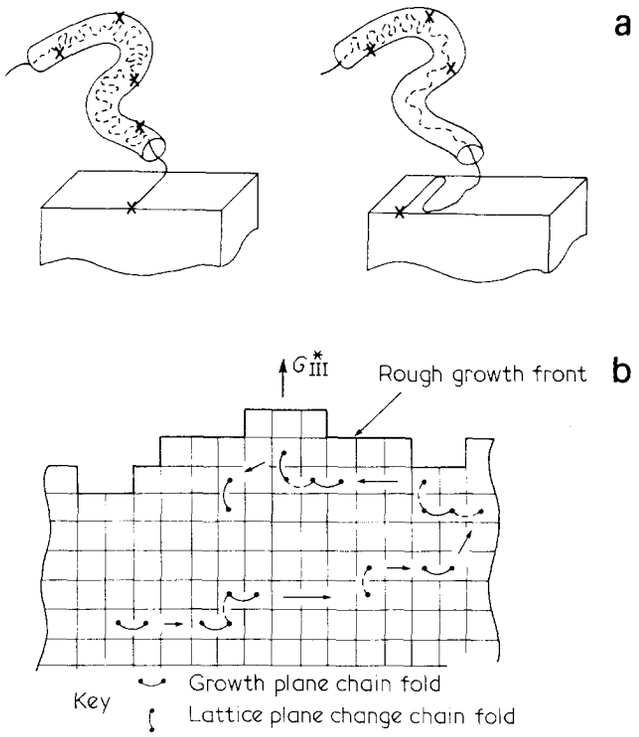

Figure 8 Formation of chain-folded cluster in Regime III by crystallization of slack (schematic): 'paired stem' variable cluster model. (a) Formation of binary cluster by reeling in of slack (schematic). Rough growth front not shown. (b) Schematic representation of typical molecular conformation in 'paired stem' variable cluster model applicable below inception of Regime III. Arrows show 'trajectory' of molecule and also indicate positions of random coil loops (not shown) between clusters. Solid curves show folds facing reader, dashed curves show folds on opposite side of lamella. Molecule exhibits $p_{tf} = 13/19 = 0.684$, $p_{nar} = 6/19 = 0.316$. Thus, while molecule has overall conformation similar to that of liquid state, a lamella formed of such molecules still has a surface with two-thirds 'tight' folds in conformity with Gambler's Ruin limits. Interlamellar link not shown

adjacent re-entry cluster size of about three, where $p_{tf} \sim 2/3$ and $p_{nar} \sim 1/3$. The simplest hypothesis that fits the facts known at present is that for a considerable temperature range beginning just below the inception of Regime III that the chain segments in the subcooled melt that participate in the small cluster formation typical of Regime III are those that represent 'slack' or 'stored length', i.e., the process involves the form of reptation that involves only a part of the pendant chain.

The concept of 'slack' or 'stored length' has been discussed by De Gennes[8], and specifically in the case of crystallization by Klein and Ball[9].

The polymer chain is imagined to be confined to a reptation tube of 'wormhole' of diameter d_0 in a kinked manner as illustrated schematically in *Figure 8*, upper diagram. The tube consists of random-coil neighbours. At various points along the tube one has 'entanglements' shown here schematically as contacts with the side of the reptation tube as (- × -). Klein and Ball suggest a tube diameter of *circa* 30 Å. What we shall postulate here is that a section of the kinked molecule in the tube can be readily extracted in a rapid manner by the force of crystallization[2] $f_c = a_0b_0(\Delta f)$ in Regime III as shown in *Figure 8a*. (This model is strongly reminiscent of that of Klein and Ball; see their *Figure 5*.) The length that is extracted in this rapid process, which we associate with the retardation factor $\exp[-U^*/R(T - T_\infty)]$, would in general correspond to the

slack length associated with a few entanglement distances. The rest of the long molecule is, in the short time scale considered, taken to be unaffected or only slightly affected. This shows that at low crystallization temperatures in Regime III that a few stems could be rapidly drawn onto the crystal face. We associate this rapid movement with a low effective activation energy process involving U^* without invoking the steady-state reptation process involving the whole pendant chain where the larger free energy of activation $Q_D^* \cong 7000$ cal mol^{-1} is applicable. (Recall that experimental growth rate studies on a number of polymers clearly show that the retardation function relevant at low temperatures is of the form $\exp[-U^*/R(T-T_\infty)]$ and not $\exp[-E^*_D/RT]$[1,17].) Accordingly, it is considered that an expression of the form of equation (23b) for G_{III}^* best reflects the physical phenomena that control the growth rate deep in Regime III.

The crystallization of the 'slack' portion of the chain is such that one might expect a rather low initial degree of crystallinity, since the slack represents only a portion of the chain. However, higher crystallinity could progressively appear in subsequent steps as new slack was developed, with the result that the overall degree of crystallinity at the end of the process may well be in the usual range, at least in the upper part of Regime III. In the longer time scale involved in Regimes I and II, the drawing in of the 'slack' region occurs first but is masked completely by the fact that much or all of the chain moves (whether it is fully reeled in or not), being opposed by the steady-state reptation activation energy Q_D^* in such a manner that the friction coefficient is proportional to the chain length. One may expect a weaker dependence on molecular weight than $1/M$ deep in Regime III.

The result that $n'_{s_{lim}} \cong 2.8$ for $\Delta T = 23.2$°C shown in equation (50a) as calculated using equation (49a) is not unexpected. A little consideration will show that when the niche separation as calculated with equation (8) approaches $\sim 3a_0$ (see *Figure 2*) so that $n'_s \sim 3$, we must also expect that $n'_{s_{lim}}$ as calculated with equation (49a) will approach ~ 3—the two calculations are essentially equivalent. It is thus not accidental in our formulation that the temperature where the minimum niche separation of $\sim 3a_0$ is achieved is also that where steady-state reptation begins to be impaired. This leads to an important insight. *The Regime* II→*Regime* III *transition not only denotes the temperature where the niche separation calculated from nucleation theory approaches its minimal value as given by the Gambler's Ruin limit as* $n'_s \cong 1/p_{nar} \cong \langle \nu_c \rangle_{min} \cong 3$, *but also represents the temperature where steady-state reptation just begins to be replaced by reptation of slack.* Some disturbance in the growth rate (probably smooth) may occur as steady state reptation gives way over a range of temperature to reptation of slack in Regime III. It is to be expected that G_{III} will convert to G_{III}^* in the process.

Earlier, we have represented the effective slack length as n^*, as shown in equation (23b). The value of n^* must be expected to be smaller than the total length of the chain. It is possible under certain assumptions to obtain a rough extimate of n^*. In viscosity measurements on molten PE, the change from M^1 to $M^{3.4}$ behaviour occurs at a molecular weight corresponding to about 300 $-CH_2-$ units[22]. The number of chain units between entanglements is customarily set at about one-half of this value, which places a lower bound on n^* of roughly 150. The actual effective slack length available is of course rather uncertain. More than one entanglement distance is almost certainly involved, which would raise n^*. However, not all of the contour length between entanglements is available, since there exists an entropically driven resistive force which would tend to diminish n^*. On balance, it is reasonable to suppose that n^* at low temperatures is probably somewhere between about 150 and 500. This is enough to allow at least paired stems connected by chain folds to be put down on the substrate; if l_g^* for PE is taken to be ~ 90 Å[1] at 80°C ($\Delta T \cong 64$°C), then two crystalline stems with an intervening chain fold require about 150 $-CH_2-$ units. Meanwhile it is clear that n^* values in the lower part of the range mentioned can come fairly close to accomodating the growth rate G_{III}^* at 80°C (see *Figure 4*). As implied earlier, we would use G_{III} rather than G_{III}^* near the II→III transition.

The above treatment of n^* is undoubtedly oversimplified, and the whole subject of the time constant and molecular details associated with the crystallization of slack deserve further consideration. In a more detailed model, we would expect n^* to depend somewhat on molecular weight, but not so strongly as to cause G_{III}^* to vary at $1/M$. Some important ideas concerning crystallization of slack have been investigated by Klein and Ball[9]. Calvert[42] has given a calculation based on elasticity theory that could be interpreted as dealing with one aspect of the crystallization of slack.

Slack and the 'paired stem' variable cluster model

Growth deep in Regime III may be regarded as closely approaching a 'worst case' for chain folding. While the force of crystallization $f_c = a_0 b_0 (\Delta f)$ is high, the retardations resulting from the necessity of reeling in slack are formidable enough to prompt one to inquire into the question of which morphological model can minimize the amount of 'reeling in' required, and still conform to the bounds on p_{nar} set by the Gambler's Ruin calculation.

One simple solution to this problem is to allow the adjacent stems to be put down on the substrate mostly in pairs well below the inception of Regime III. Then the 'paired stem' version of the variable cluster model suggested by Guttman *et al.*[27,30] in connection with SANS studies would appear to be a plausible molecular morphology. This model is illustrated schematically in *Figure 8b*. The molecular morphology is very similar to that shown in *Figure 7*, except that there are a larger number of isolated pairs of stems. Many of the paired stems are connected to each other by random flights. For the sample trajectory shown in *Figure 8*, $p_{tf} = 13/19 = 0.684$, and $p_{nar} = 6/19 = 0.316$. Because of the almost equal number of growth plane and lattice plane change chain folds, the fold surface exhibits considerable 'fold vector' disorder. Nevertheless, the lamellar surface is over two-thirds 'tight' folds. The model exhibits properties that are essentially identical to the general variable cluster model, i.e., it gives a liquid-like radius of gyration where $R_g \propto M^{\frac{1}{2}}$, has p_{tf}, p_{ar} and p_{nar} in the permissible range, and exhibits no density anomaly. We would expect the growth rate to be given by an expression of the general form of equation (23b) for G_{III}^*.

The admixture of normal and lattice change chain folds depicted in *Figure 8b* is such as to preclude sectorization. Observable sectorization effects would only appear when

fairly long runs of adjacent folds were present, such as may occur at sufficiently high crystallization temperatures.

The foregoing picture, while lacking full detail, is nevertheless consistent with the rapid crystallization rates observed deep in Regime III in PE wherein a few adjacent stems can be drawn down onto the substrate, probably in the 'paired stem' variable cluster morphology, in a relatively low activation energy process at temperatures where the higher activation energy steady state-reptation process evident in Regime I and II and the first part of Regime III is inoperative. The process is to be viewed as renewable in the sense that new slack can be formed after a suitable interval in polymers of normal molecular weight.

Crystallinity, slack and rapid quenching. Effect of high molecular weight

The model suggests that the initial crystallinity deep in Regime III will be lower than that in Regimes I and II, or at the beginning of Regime III, though renewal of slack may mitigate this effect. Further, the model requires that the growth process will cease completely at T_{∞} (see equation (23b) for G^{*}_{III}), so that sufficiently rapid quenching to temperatures below T_{∞} should result in an amorphous polymer. Experiments by Cutter, Hendra, and Sang[19] show that amorphous films can be formed by very rapid quenching of thin films of slightly branched PE to cryogenic temperatures[44]. Crystallization of such films begins at about 180 K on warming. This suggests that T_{∞} for (slightly branched) PE may be in the vicinity of 180 K, which is only slightly lower than the nominal value $T_{\infty} = 201$ K used elsewhere in this paper.

The aforementioned experiments imply the presence of considerable chain mobility in undercooled PE down to quite low temperatures. Geil and coworkers[43] have previously gathered a considerable body of evidence pointing to this conclusion. The concept of reptation of slack, with renewal, is consistent with these findings.

Up to this point, we have mainly discussed PE specimens with a molecular weight of $\sim 2 \times 10^4$ to $\sim 2 \times 10^5$. It is of interest to note the effects that may occur in specimens of very high molecular weight. In such high molecular weight specimens, there will exist a strong tendency for the very long molecules to nucleate on many different lamellar crystallites. Then the crystallization that took place in this highly constrained system could be pictured as tending to involve mainly the slack, which in this case would be difficult to renew because most of the chains in the amorphous regions would be attached to two or more lamellae. Here one may expect a failure of the simple $G \propto 1/n \propto 1/M$ law and a definite reduction in the degree of crystallinity. It is well known that the crystallinity is reduced in high molecular weight PE[45] beginning at about 1 or 2×10^5. Such constraints might also limit the ability of the system to form large objects such as spherulites or axialites. We note in this connection that in our work on spherulite growth rates in PE fractions[3] that no such objects, including 'irregular' spherulites, could be seen in an optical microscope for specimens exceeding $M_w \cong 8 \times 10^5$, even though there was clear evidence of the presence of crystallinity of a lamellar character. The crystallites in such specimens were evidently very small. Another consequence of the constraints on steady-state reptation in such a system could be the appearance of some aspects of Regime III type behaviour in the temperature range where Regime II behaviour was seen at the same ΔT in specimens of moderate molecular weight. Though samples of somewhat higher and lower molecular weight exhibited intermediate values, the K_g values of the 'irregular' spherulites in specimens $M_w = 2.66 \times 10^5$ ($M_z = 4.82 \times 10^5$) and $M_w = 3.23 \times 10^5$ ($M_z = 5.01 \times 10^5$) are quite close to those expected for Regime III behaviour, even though the temperature and undercooling range was that where Regime II behaviour clearly occurred in specimens of moderate molecular weight[3]. Accordingly, the Regime III effect may not always be confined to rather large undercoolings, especially in specimens of very high molecular weight. Further, the variable cluster morphology, with the long chains participating in many microlamellae, and with the majority of the stems in the small clusters being largely the result of the crystallization of slack, may well be a close approximation to the true situation in linear PE of very high molecular weight even under normal conditions of crystallization.

It is worth noting that in systems where reptation (including the reeling in of slack) is strongly impaired, e.g., by numerous branches[44], the possibility exists that the system will not be able to form chain folds on quenching, but will only be able to crystallize, if it does so at all, by the accretion of isolated stems. If in such a case the crystallites are lamellar, it is to be anticipated that they will be of the fringed micellar, random switchboard, or 'Erstarrungsmodell' type *but with the important modification that the stems in the crystal will exhibit a very large tilt* ($> 70°$) *from the perpendicular to the lamellar surface.* Highly branched PE may for instance exhibit such behaviour on being quench-crystallized. (If reptation were possible, chain folding would occur for kinetic reasons, since $\sigma_{e(\text{fringed micelle})}$ is greater than $\sigma_{e(\text{fold})}$.) Alternatively, the system may form numerous fringed micellar crystallites of very small dimensions, each containing a relatively small number of stems. The crystallites would tend to have rounded ends in order to minimize the end surface free energy and to avoid a density anomaly.

Melt temperature 'memory' effects

Finally, we remark on the possibility of memory effects that might occur from heating a polymer to different melt temperatures T_1 (that are above T_m°) prior to crystallization at T_x. Such effects are absent in most polymers, including PE, when T_x corresponds to growth temperatures near the melting point, where crystallization is relatively slow. Thus, in PE, the crystallization rate of a given specimen in Regimes I or II depends only on T_x, and not on T_1 or the residence time at T_1[3]. We do not expect an effect of varying T_1 in the upper part of Regime III in PE and we have accordingly not attempted to include the effect of varying T_1 in our theoretical development. However, very rapid quenching from various T_1 to a low fixed T_x may lead to crystallization at that T_x which shows a memory effect of the different molecular conformations in the liquid corresponding to the various T_1 values employed. Cutter *et al.*[19] have obtained results for slightly branched PE that was very rapidly quenched to a fixed cryogenic T_x that exhibited different lamellar thicknesses as T_1 was varied. This may imply the existence of a liquid state memory effect in crystallization experiments carried out under such extreme conditions. The observation of such memory effects does not invalidate the nucleation

theory approach for estimating the initial stem length l_g^*, but does complicate the determination of (Δf) in $l_g^* = 2\sigma_e/(\Delta f) + C_2$[46].

SUMMARY AND CONCLUSIONS

(1) Nucleation theory has been applied in a straightforward manner to calculate the mean separation of the niches on the substrate in Regime II. The result is that the niche separation rapidly approaches the stem width at an undercooling corresponding to a temperature well below the Regime I→Regime II transition. Regime III behaviour is predicted to begin at a temperature corresponding to that where the niche separation corresponds approximately to the width $n_s' = 3$ stems. The Regime III transition in PE is postulated to begin at about $\sim 121°C$ ($\Delta T \cong 23°C$) though one modification of the theory suggests it may be slightly lower. (The Regime I→Regime II transition is $\Delta T \sim 16°C$.) The onset of Regime III is denoted in general by an upswing in the growth rate with lowering temperature because $G_{III} \propto i$ and $G_{II} \propto i^{\frac{1}{2}}$.

(2) Explicit formulae are developed for Regime III kinetics, including the pre-exponential factors, for both PE and POM. Expressions are also given for Regimes I and II to complete the picture.

(3) A comparison is made of theory and experiment for PE and POM. In the case of PE the requisite low temperature growth rate data are somewhat limited in scope, but still sufficient to firmly indicate the reality of the Regime III effect. The more extensive growth rate data on POM clearly reveal the presence of both Regimes II and III, and exhibit almost precisely the anticipated change of a factor of two in the K_g values at the II→III transition. This shows that $G_{II} \propto i^{\frac{1}{2}}$ and $G_{III} \propto i$ as expected. The predicted upswing in growth rate as Regime III is entered at $\Delta T \geqslant 40°C$ appears clearly. An expression for Regime I behaviour in POM is given, but could not be tested since growth rate data at sufficiently high temperatures were not available. It is shown for POM that the pre-exponential factors for Regimes II and III have nearly the correct ratio, and that the initial lamellar thickness predicted from the σ_e value derived from the kinetics is consistent with experiment. The successful prediction of the Regime II→III transition and its experimental verification in PE and POM provides a considerable body of evidence favouring the reality of the concept that 'niches' are active sites for the addition of stems in the substrate completion process[47].

(4) A discussion is given of the molecular morphology expected in Regime III. Using considerations based on the small niche separation characteristic of Regime III, and the requirement derived from the Gambler's Ruin problem that the degree of non-adjacent re-entry p_{nar} is restricted to values equal to or less than about one-third, it is shown that the variable cluster model is appropriate to Regime III. Application of $p_{nar} \leqslant \sim 1/3$ assures that no inadmissibly large buildup of segment density at the lamellar surface will occur, as happens in the case of the random switchboard model. In the variable cluster model, runs of stems with adjacent re-entry of varying size, but averaging close to three stems, are laid down, interspersed with non-adjacent re-entry type of events that are random flights which lead to loops and interlamellar links. The growth front in Regime III is extremely rough because of the intense multiple nucleation.

(5) It is noted that the variable cluster model is not only consistent with what is known about the kinetics of Regime III, but also with information on the conformation of the polymer chains in quench-crystallized PED–PED mixtures as revealed by neutron scattering. In particular, the neutron scattering data yield a mean cluster size of $\langle v_c \rangle \sim 3$, and by this and other routes defines the mean niche separation as being between about $2.5a_0$ and $4a_0$, i.e., $n_s' \sim 3$. This substantiates the effective substrate length $L' = n_s' a_0$ with $n_s' \sim 3$ employed in the calculations on the kinetics of Regime III. The radius of gyration R_g for the variable cluster model is essentially the same as that of the liquid, and varies as $M^{\frac{1}{2}}$, even though the probability of regular folding is close to two-thirds. It is well known that quench-crystallized PEH–PED mixtures, which correspond to Regime III crystalization, give R_g values that correspond to these predictions. The variable cluster model is shown to accommodate the degree of crystallinity characteristic of quench-crystallized PE. It should be recognized that Regime III crystallization, as epitomized by quench-crystallized PE, represents a 'worst case' for regular chain-folding, and that the concommitant variable cluster model can give way to models with longer runs of adjacent stems under different crystallization conditions. As noted in the text, *i*-PS can exhibit rather long runs of adjacent stems ('central core' or 'ACA' model) under suitable conditions of melt crystallization.

(6) It is demonstrated for PE that the steady-state reptation process leading to the $\sim 1/M$ dependence of the growth rate in Regimes I and II is sufficiently rapid to accommodate the formation of the small clusters characteristic of Regime III crystallization near its inception. This steady-state reptation process is, however, shown to be too slow at lower temperatures, and it is suggested that it is the 'slack' portions of the pendant molecules that rapidly crystallize in the body of Regime III. This is predicted to reduce somewhat the dependence of the growth rate on molecular weight, and to be associated with a retardation function of the form $\exp[-U^*/R(T - T_\infty)]$ that in effect represents a lower effective activation energy in the transition region than does the expression $\exp(-Q_D^*/RT)$ characteristic of the steady-state reptation process. The corresponding expression for the growth rate at low temperatures appears to be approximately correct. At temperatures somewhat below the inception of Regime III, where many of the stems that are put down respresent crystallization of slack, the molecular morphology is suggested to be similar to that of the 'paired stem' version of the variable cluster model.

(7) Comments are presented on the structures that might develop with branching and very rapid quenching. It is also noted that in specimens of very high molecular weight, the growth process may be mainly the result of the reeling in of slack. Liquid state 'memory' effects in specimens rapidly quenched to crystallization temperatures deep in Regime III are discussed.

(8) We now address what has been done in broader terms. The approach presented in this and a preceding paper[2] conjoins nucleation theory, reptation theory, regime theory, and the Gambler's Ruin treatment in an attempt to provide a comprehensive and consistent picture of the formation of chain-folded lamellae from a polymer melt over a wide range of crystallization temperature and molecular weight. (Low molecular weight

polymer is excluded.) Reptation theory combined with nucleation theory and Regime theory gives the rate of growth as a function of temperature in Regimes I and II, and simultaneously predicts the initial lamellar thickness. Steady state reptation provides the mechanism by which a polymer molecule or portion thereof can be extracted from the interentangled melt and reeled onto the substrate by the force of crystallization, and also is the source of the dependence of growth rate on molecular weight in these Regimes. The niche separation theory adjunct to Regime II demands that Regime III begin at a temperature where that separation becomes irreducible. Steady state reptation is rapid enough to allow nucleation and substrate completion in Regimes I and II, and at first in Regime III, but is not viable as a transport mechanism in the main body of Regime III where slack must be invoked to permit at least paired stems to enter the growth front. Application of the Gambler's Ruin constraints greatly limits the degree of non-adjacency even when many closely spaced niches are present on the growth front as in Regime III. (Conformity to the restraints given by Gambler's Ruin assures that no density anomaly will occur at the lamellar surface because of an excessive number of emergent random-coil entities per unit area.) The closely spaced niches act to minimize the size of the chain-folded clusters in Regime III, but the restrictions of non-adjacent re-entry imposed by Gambler's Ruin force the chain-folded clusters to contain an average of *circa* three stems. The non-adjacent re-entry events associated with the clusters account for the amorphous component, which consists of loops on a given lamella, and an occasional interlamellar link. Thus, a straightforward application of nucleation theory (with reptation) and Regime theory, combined with the Gambler's Ruin requirements, leads unerringly to the variable cluster model as the dominant molecular morphology in Regime III. The Gambler's Ruin conditions require for approximately vertical stems that the lamellar surface consist of about two-thirds 'regular' or 'tight' folds. In the simplest possible terms, *the chain-folded lamellar morphology so prevalent in melt-crystallized polymers is fundamentally a result of nucleation kinetics operating in conjunction with the necessity of avoiding a density paradox at the lamellar surface resulting from an excessive concentration of emergent volume-filling random coil type structures.*

ACKNOWLEDGEMENT

The author wishes to especially thank Dr P. J. Barham of the University of Bristol for helpful communications and permission to use his unpublished data on the growth rate of PE at low temperatures. Special thanks are also due Drs C. M. Guttman and E. A. DiMarzio of NBS for numerous critical discussions and much encouragement, and to Drs G. T. Davis, F. Khoury, D. Reneker, L. Frolen and G. S. Ross of NBS for helpful review and comment. The author gratefully acknowledges a discussion with Prof. R. H. Boyd of the University of Utah concerning the chain energetics of POM.

REFERENCES

1 Hoffman, J. D., Davis, G. T. and Lauritzen, Jr., J. I. in 'Treatise on Solid State Chemistry', Ed. N. B. Hannay (Plenum Press, New York, 1976), Vol. 3, Ch. 7

2 Hoffman, J. D. *Polymer* 1982, **23**, 656

3 Hoffman, J. D., Frolen, L. J., Ross, G. S. and Lauritzen Jr., J. I. *J. Res. Natl. Bur. Stand.* 1975, **79A**, 671

4 Guttman, C. M., DiMarzio, E. A. and Hoffman, J. D. *Polymer* 1981, **22**, 1466 (cubic lattice case). See also Guttman, C. M. and DiMarzio, E. A. *Macromolecules* 1982, **15**, 525 (rotational isomeric model case)

5 Pelzbauer, Z. and Galeski, A. *J. Polym. Sci., C*, 1972, **38**, 23

6 Barham, P. J., Jarvis, D. A. and Keller, A. *J. Polym. Sci. Polym. Phys. Edn.* 1982, **20**, 0000

7 Schelten, J., Ballard, D. G. H., Wignall, G. D., Longman, G. and Schmatz, W. *Polymer* 1976, **17**, 751

8 deGennes, P. G. *Macromolecules* 1976, **9**, 587; also *J. Chem. Phys.* 1971, **55**, 572

9 Klein, J. and Ball, R. C. *Disc. Faraday Soc.* No. 68, 1979, 198

10 Hoffman, J. D., Guttman, C. M. and DiMarzio, E. A. *Disc. Faraday Soc.* No. 68, 1979, 177

11 Lauritzen Jr., J. I. *J. Appl. Phys.* 1973, **44**, 4353; for another derivation see Frank, F. C. *J. Crystal Growth* 1974, **18**, 111

12 Hoffman, J. D. *Disc. Faraday Soc.* No. 68, 1979. See discussion remarks on p. 378

13 Klein, J. and Briscoe, B. J. *Proc. Roy. Soc. (London)*, 1979, **A365**, 53

14 Phillips, P. J. *Polym. Prepr.* 1979, **20**, 483

15 Frank, F. C. and Tosi, M. *Proc. Roy. Soc. (London)*, 1961, **A263**, 323

16 Lauritzen, Jr., J. I. and Passaglia, E. *J. Res. Natl. Bur. Stand.* 1967, **71A**, 261

17 Suzuki, T. and Kovacs, A. J. *Polym. J. (Jpn.)* 1970, **1**, 82

18 Davis, G. T. and Eby, R. K. *J. Appl. Phys.* 1973, **44**, 4274

19 There is considerable discussion concerning the correct value of T_g for PE. Lower values than that used here have been suggested. For example, Cutter, D. J., Hendra, P. J. and Sang, R. D. [*Disc. Faraday Soc.* No. 68, 1979, 320] suggest an upper limit of 180 K for T_g on the basis of the temperature of the onset of crystallization on re-warming of glassy specimens of slightly branched PE obtained by very rapid quenching to cryogenic temperatures. We would expect crystallization to begin just above $T_c = T_g - 30$ K (as opposed to just above T_g) which suggests $T_c \cong 180$ K and $T_g \cong 210$ K, which is not seriously at variance with the T_c and T_g values that we have employed. In any event, equation (23b) can readily be adjusted to other T_c values with no basic change in physical interpretation as regards Regime III

20 There are limitations on the growth rate that may be reasonably predicted by the present type of theory. A growth rate G is associated with a relaxation time for the laying down of n'_s stems of $\tau = n'_s b_0/G = (i' a_0)^{-1}$. For $n'_s \sim 3$ and $b_0 = 4.55 \times 10^{-8}$ cm, this comes to $\tau \sim 1.4 \times 10^{-7}$ cm/G(cm s^{-1}). The maximum conceivable growth rate is $G \sim b_0(kT/h)$ or 3.4×10^5 cm s^{-1} at 80 °C. This gives $\tau \sim 4 \times 10^{-13}$ s which is in the order of what one would expect. We consider that the present type of theory for Regime III should not be pressed to the point that relaxation times much shorter than 10^{-8} s are involved, which limits G_{III} and G_{III}^* to the order of magnitude of 10 cm s^{-1}. At shorter relaxation times, i.e., at higher G values, it would be appropriate to question the steady-state approximation, and certain other assumptions such as the full availability of the configurational path degeneracy P_0 in such a rapid process

21 Private communication from P. J. Barham, University of Bristol, UK

22 Ferry, J. D. 'Viscoelastic Properties of Polymers' 2nd Edn. (1970), John Wiley and Sons, New York

23 Rybnikar, F. *Collect. Czech. Chem. Commun.* 1966, **31**, 4080

24 Amano, T., Fischer, E. W. and Hinrichsen, G. *J. Macromol. Sci.-Phys.* 1969, **B3 (2)**, 209

25 In a previous publication (ref. 1) considerably lower σ_e and q values were quoted for melt-crystallized POM than have been given in the present paper. This can be traced directly to our use in ref. 1 of a much lower melting point ($T_m^\circ = 186$°C) in the analysis of the growth rate data. Estimates of T_m° in this vicinity are readily to be found in the literature. However, the work of Amano, Fischer and Hinrichsen (ref. 24) not only verifies by direct experiment that a melting point near 200°C is correct for extended-chain hexagonal POM, but also describes the phenomena near 185°C that had apparently been mistaken by others for the melting point of large extended-chain crystallites. The work of Rybnikar (ref. 23) further verifies that T_m° for the hexagonal form of melt-crystallized POM is in the vicinity of 200°C, and in addition shows by the T_m' *versus* $1/l$ thermodynamic method that σ_e for hexagonal POM is between about 171 and 205 erg cm^{-2}. (Recall that here we have found $\sigma_e = 183$ erg cm^{-2} by a

kinetic analysis using $T_m^\circ = 198.3°C$.) Thus the situation seems clearly resolved in favour of the higher melting point and higher σ_e and q value in the case of melt-crystallized hexagonal POM

26 Ushida, T., Kurita, Y. and Kubo, M. *J. Polym. Sci.* 1956, **19**, 365

27 Guttman, C. M. *Disc. Faraday Soc.* No. 68, 1979. Discussion remarks on p. 457

28 Frank, F. C. in 'Growth and Perfection of Crystals' (Proceeding of an International Conference on Crystal Growth held at Cooperstown, New York, August 27–29, 1958), Ed. Doremus, Roberts, and Turnbull (John Wiley, New York, 1958), discussion remarks on pp. 529 and 530

29 Frank, F. C. *Disc. Faraday Soc.* No. 68, 1979, 7

30 Guttman, C. M., Hoffman, J. D. and DiMarzio, E. A. *Disc. Faraday Soc.* No. 68, 1979, 297

31 Yoon, D. Y. and Flory, P. J. *Polymer* 1977, **18**, 509

32 Guttman, C. M., DiMarzio, E. A. and Hoffman, J. D. *Polymer* 1981, **22**, 597

33 Sadler, D. M. *Disc. Faraday Soc.* No. 68, 1979. Discussion remarks on p. 106

34 Guttman, C. M. *Disc. Faraday Soc.* No. 68, 1979. Discussion remarks on p. 433

35 In reference 30, Guttman *et al.* report the number of folds/cluster for various models. The value of $\langle v_c \rangle$ is (folds/cluster) + 1

36 Stamm, M. *J. Polym. Sci. Polym. Phys. Edn.* 1982, **20**, 235

37 Wignall, G. D., Mandelkern, L., Edwards, C. and Glotin, M. *ibid.* 245

38 Guenet, J. M., Picot, C. and Benoit, H. *Disc. Faraday Soc.* No. 68, 1979, 251

39 Yoon, D. Y. and Flory, P. J. *Disc. Faraday Soc.* No. 68, 1979, 288

40 Flory, P. J. and Yoon, D. Y. *Nature* 1978, **272**, 226

41 Backman, D. K. and DeVries, K. L. *J. Polym. Sci. A-1* 1969, **7**, 2125

42 Calvert, P. *J. Polym. Sci. Polym. Phys. Edn.* 1979, **17**, 1341

43 Lam, R. and Geil, P. H. *Science* 1974, **205**, 1388; Geil, P. H. *Disc. Faraday Soc.* No. 68, 1979, discussion remarks on p. 440

44 It has been pointed out by DeGennes [*Disc. Faraday Soc.* No. 68, 1979, discussion remarks on p. 381] that reptation may be impaired by branches. This may account for the apparent requirement that a small amount of branching be present to allow amorphous PE to be formed, as noted by Cutter *et al.* (ref. 19). It is these observations that led us to suggest in the text that if a considerable amount of branching were present in PE that difficulty might be encountered in crystallizing such material with chain folding because of the retardation to reptation

45 Mandelkern, L. *Disc. Faraday Soc.* No. 68, 1979, 310

46 If it is assumed that the fraction of *gauche* states at the various T_1 values employed is 'frozen in' by sufficiently rapid quenching to a low crystallization temperature, it is possible to predict that the driving force (Δf) at that low temperature will be a function of T_1, the larger (Δf) values being associated with the higher T_1 values. Then through the relation $l_g^* \cong 2\sigma_e/(\Delta f) + C_2$ from nucleation theory, it is readily seen that the smaller initial lamellar thickness l_g^* is then associated with the higher T_1 value. This is in qualitative accord with the experiments on PE of Cutter *et al.*[19], which involved very rapid quenching to cryogenic temperatures. (It should be noted that Δf 'with the normal fraction of *gauche* states is not given by equation (3a) of the text at very low temperatures; see pp. 540–541 of ref. 1.) In the usual 'slow' experiment at a normal crystallization temperature, the fraction of *gauche* states and hence (Δf) would be solely a function of T_x, and no memory effect of T_1 would be seen. This is consistent with experiments on PE fractions carried out in Regimes I and II[3]

47 Doubt has been expressed concerning whether 'niches' are favoured sites for the attachment of polymer stems on a growth front (see Wunderlich, B. *Disc. Faraday Soc.* No. 68, 1979, 239). Otherwise, the belief that niches are active sites for the attachment of stems appears to be widely accepted. If niches were not operative on the substrate, neither the existence of the Regime I→II nor most especially the Regime II→III transition could be predicted or understood. In the light of this development, the experimental evidence cited by Wunderlich as disfavouring the niche concept should be reconsidered